Article

Molecular Cell

Chromodomain Protein CDYL Acts as a Crotonyl-CoA Hydratase to Regulate Histone Crotonylation and Spermatogenesis

Graphical Abstract

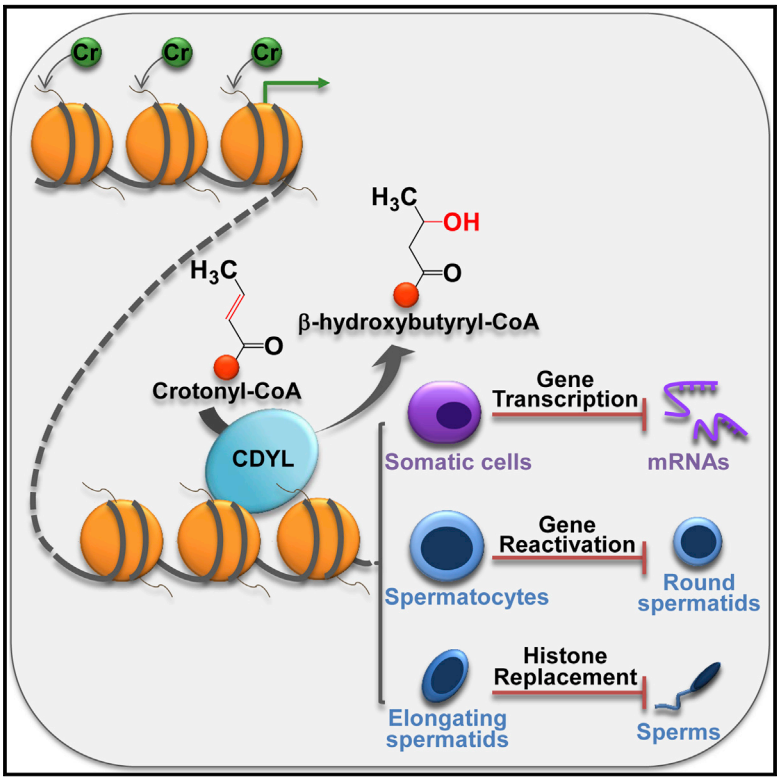

Highlights

- The chromodomain Y-like protein CDYL negatively regulates histone crotonylation
- CDYL acts on crotonyl donor as a crotonyl-CoA hydratase
- CDYL-regulated histone crotonylation is linked to its corepressor function
- CDYL-regulated histone crotonylation is important for mammalian spermatogenesis

Authors

Shumeng Liu, Huajing Yu, Yongqing Liu, ..., Zhongyi Cheng, Jing Liang, Yongfeng Shang

Correspondence

liang_jing@hsc.pku.edu.cn (J.L.), yshang@hsc.pku.edu.cn (Y.S.)

In Brief

Liu et al. demonstrate that the chromodomain Y-like protein CDYL acts as a crotonyl-CoA hydratase to negatively regulate histone crotonylation. This activity is intrinsically linked to the transcription repression function of CDYL and is implemented in reactivation of sex chromosome-linked genes and histone replacement during spermatogenesis.

Liu et al., 2017, Molecular Cell 67, 1–14
September 7, 2017
http://dx.doi.org/10.1016/j.molcel.2017.07.011

CellPress

Please cite this article in press as: Liu et al., Chromodomain Protein CDYL Acts as a Crotonyl-CoA Hydratase to Regulate Histone Crotonylation and Spermatogenesis, Molecular Cell (2017), http://dx.doi.org/10.1016/j.molcel.2017.07.011

Molecular Cell
Article

Chromodomain Protein CDYL Acts as a Crotonyl-CoA Hydratase to Regulate Histone Crotonylation and Spermatogenesis

Shumeng Liu,[1,2] Huajing Yu,[1] Yongqing Liu,[1] Xinhua Liu,[2,3] Yu Zhang,[1] Chen Bu,[4] Shuai Yuan,[1] Zhe Chen,[1] Guojia Xie,[1] Wanjin Li,[1] Bosen Xu,[1] Jianguo Yang,[1] Lin He,[1] Tong Jin,[1] Yundong Xiong,[1] Luyang Sun,[1] Xiaohui Liu,[5] Chunsheng Han,[6] Zhongyi Cheng,[4] Jing Liang,[1,*] and Yongfeng Shang[1,2,3,7,*]

[1]Key Laboratory of Carcinogenesis and Translational Research (Ministry of Education), Department of Biochemistry and Molecular Biology, School of Basic Medical Sciences, Peking University Health Science Center, Beijing 100191, China
[2]Department of Biochemistry and Molecular Biology, School of Basic Medical Sciences, Capital Medical University, Beijing 100069, China
[3]Department of Biochemistry and Molecular Biology, School of Basic Medical Sciences, Tianjin Medical University, Tianjin 300070, China
[4]Jingjie PTM BioLab (Hangzhou), Co. Ltd., Hangzhou 310018, China
[5]School of Life Sciences, Tsinghua University, Beijing 100084, China
[6]State Key Laboratory of Reproductive Biology, Institute of Zoology, Chinese Academy of Sciences, Beijing 100101, China
[7]Lead Contact
*Correspondence: liang_jing@hsc.pku.edu.cn (J.L.), yshang@hsc.pku.edu.cn (Y.S.)
http://dx.doi.org/10.1016/j.molcel.2017.07.011

SUMMARY

Lysine crotonylation (Kcr) is a newly identified histone modification that is associated with active transcription in mammalian cells. Here we report that the chromodomain Y-like transcription corepressor CDYL negatively regulates histone Kcr by acting as a crotonyl-CoA hydratase to convert crotonyl-CoA to β-hydroxybutyryl-CoA. We showed that the negative regulation of histone Kcr by CDYL is intrinsically linked to its transcription repression activity and functionally implemented in the reactivation of sex chromosome-linked genes in round spermatids and genome-wide histone replacement in elongating spermatids. Significantly, *Cdyl* transgenic mice manifest dysregulation of histone Kcr and reduction of male fertility with a decreased epididymal sperm count and sperm cell motility. Our study uncovers a biochemical pathway in the regulation of histone Kcr and implicates CDYL-regulated histone Kcr in spermatogenesis, adding to the understanding of the physiology of male reproduction and the mechanism of the spermatogenic failure in *AZFc* (Azoospermia Factor c)-deleted infertile men.

INTRODUCTION

Histone modifications represent important mechanisms of the epigenetic regulatory network that dictates a wide range of biological processes including replication, transcription, and DNA damage repair. Recently, the variety of histone modification has expanded and a group of related histone lysine acylations including butyrylation, crotonylation, malonylation, propionylation, and succinylation have been identified (Sabari et al., 2017). While chemically analogous to the well-studied histone acetylation, the biological functions and the "writer," "reader," and "eraser" responsible for the addition, recognition, and removal of these acylations are yet to be identified.

Since the discovery of histone lysine crotonylation (Kcr) (Tan et al., 2011), several regulatory enzymes for histone Kcr have been described. For the addition of histone Kcr, it is recently reported that the well-studied transcriptional coactivator and histone acetyltransferase (HAT) p300 possesses histone crotonyltransferase activity (Sabari et al., 2015). For the removal of histone Kcr, it is reported that HDAC3 in complex with nuclear receptor corepressor 1 (NCoR1) had a measureable decrotonylase activity *in vitro*, albeit at a significantly lower rate than its deacetylase activity (Madsen and Olsen, 2012). It was also shown that SIRT1, SIRT2, and SIRT3 could act as decrotonylases (Bao et al., 2014; Feldman et al., 2013). Clearly, the regulatory mechanisms and enzymes involved in the negative regulation of histone Kcr need further investigation, especially considering that HDAC3 and SIRT1/2/3 are all well-recognized histone deacetylases.

Chromodomain Y-like (CDYL) protein, containing an N-terminal chromodomain and a C-terminal enoyl-coenzyme A hydratase/isomerase catalytic domain (also known as CoA pocket or CoAP), has been implicated in epigenetic regulation and transcription repression (Caron et al., 2003; Lahn and Page, 1999). Human CDYL belongs to a family of chromodomain Y-related proteins, which contain testis-specific CDY and ubiquitously expressed CDYL and CDYL2 (Dorus et al., 2003; Lahn et al., 2002). In mice, the CDY-related gene family consists of two autosomal members, Cdyl and Cdyl2. Cdyl gene produces a testis-specific 2.8 kb transcript and a ubiquitously expressed 3.6 kb transcript; the two differ only in their 3′-untranslated regions and thus encode the same protein (Lahn and Page, 1999; Li et al., 2007). Evolutionarily, mouse Cdyl and human CDYL proteins share 93% overall identity, with even greater similarities in the chromo and CoAP domains (Lahn and Page, 1999). Remarkably, human *CDY* is mapped to *AZFc* (Azoospermia Factor c), a region of the Y chromosome that is frequently deleted in infertile men

who suffer from spermatogenic failure (Kuroda-Kawaguchi et al., 2001; Lahn et al., 2002; Vogt et al., 1996), suggesting that *CDY* might be critically involved in spermatogenesis.

It is believed that CDYL reads histone H3 lysine 9 trimethylation (H3K9me3) and H3K27me3 through its chromodomain (Kim et al., 2006; Vermeulen et al., 2010) and interacts with PRC2, generating a positive feedback loop to facilitate the propagation of H3K27me3 along chromatin (Zhang et al., 2011). In contrast, the function of the CoAP domain of the CDY family proteins is poorly defined. Although CDY proteins have been reported to possess HAT activity toward histone H4 *in vitro* (Lahn et al., 2002), the responsible domain was not assigned. More importantly, a transcription corepressor exhibiting HAT activity is extremely puzzling. Indeed, a later study reported that the CoAP domain of CDYL is able to bind coenzyme A and recruit HDAC1 and HDAC2 (Caron et al., 2003), and crystallographic studies revealed that the structures of the CoAP domain of CDY proteins exhibit no similarity to that of any known HATs, instead resembling that of the crotonase superfamily, a group of divergently related enzymes with a common feature of stabilizing an enolate anion intermediate derived from an acyl-CoA substrate (Wu et al., 2009). Clearly, the catalytic activity of CDYL remains to be elucidated.

We report here that CDYL acts as a crotonyl-CoA hydratase to negatively regulate histone Kcr. We demonstrated that CDYL-catalyzed downregulation of histone Kcr is intrinsically linked to its transcription repression activity and functionally implemented in spermatogenesis by influencing the reactivation of sex chromosome-linked genes in round spermatids and histone replacement in elongating spermatids. We generated *Cdyl* transgenic mice and found that the epididymal sperm count, sperm cell motility, and male fertility of these animals are all compromised.

RESULTS

CDYL Inhibits Both Nonenzymatic and Enzymatic Histone Kcr *In Vitro*

The fact that CDY proteins contain a CoA-binding pocket (Caron et al., 2003) and the observation that CDYL possesses a HAT activity *in vitro* (Lahn et al., 2002) prompted us to investigate whether CDY proteins might possess histone crotonyltransferase activity. Since previous studies indicate that histone Kcr could occur nonenzymatically and can be regulated by the concentration of crotonyl-CoA (Sabari et al., 2015), we thus first incubated native calf thymus histones (CTHs) with increasing amount of crotonyl-CoA. Western blotting detected a marked increase in the level of histone Kcr, whereas few changes in histone acetylation were detected when equal amount of acetyl-CoA was added in the reaction (Figure 1A), indicating that histone Kcr could occur nonenzymatically. We then incubated bacterially purified recombinant human CDYL with native CTH in the presence of crotonyl-CoA. Surprisingly, contrary to what was expected, addition of CDYL resulted in a dose-dependent decrease, rather than an increase, in histone Kcr (Figure 1B). Analogously, inclusion of recombinant CDY or CDYL2 in the reaction also led to a reduction of histone Kcr (Figure 1C). Similar inhibitory effect of nonenzymatic histone Kcr was also observed when recombinant CDYL was substituted by baculovirally expressed CDYL (Figure 1D) or when CTHs were substituted by recombinant *Xenopus* histone octamers (Figure 1E). We further examined whether CDYL could affect p300-catalyzed histone Kcr *in vitro*. While baculovirally expressed p300 could efficiently catalyze Kcr toward recombinant histone octamers, inclusion of recombinant CDYL to the reaction greatly inhibited p300-catalyzed histone Kcr (Figure 1F). Together, these data indicate that CDY family proteins negatively regulate histone Kcr *in vitro*.

CDYL Negatively Regulates Histone Kcr in Cells

Given that CDYL is a better-studied and ubiquitously expressed member of the CDY family (Dorus et al., 2003) and histone Kcr is involved in epigenetic regulation in a generalized, not tissue-specific, way (Sabari et al., 2015; Tan et al., 2011), we thus focused the rest of our study on CDYL. Knockdown of CDYL in HeLa cells with its specific siRNAs was associated with an evident increase in total histone Kcr level and a more pronounced increase in the level of Kcr at H2BK12, H3K9, H3K27, and H4K8, as measured by immunoblotting of acid-extracted histones (Figure 2A). Moreover, immunoblotting of chromatin histones isolated from a CDYL knockout (CDYL-KO) HeLa cell line that we generated using TALEN technology also detected an overt elevation of histone Kcr (Figure 2B), supporting a notion that CDYL inhibits or negatively regulates histone Kcr.

To further substantiate these observations, we utilized an integrated approach of SILAC labeling and affinity enrichment followed by high-resolution liquid chromatography-tandem mass spectrometry (LC-MS/MS) to quantify the differential levels of histone Kcr in CDYL-KO versus wild-type HeLa cells (Figure 2C). Among a total of 36 crotonylated core histone lysine sites identified and quantified, eight sites showed significant increases in crotonylation level in CDYL-KO cells (Figure 2D). For example, LC-MS/MS detected a 2.6-fold increase in H2BK12cr in CDYL-KO cells (Figure S1). The remaining sites exhibited no significant changes in Kcr level (Figure 2D). These results further support the proposition that CDYL negatively regulates histone Kcr in cultured cells.

Both the Chromodomain and CoAP Domain of CDYL Are Required for Its Negative Regulation of Histone Kcr

As stated before, CDYL is characterized as a transcription corepressor that targets chromatin through its N-terminal chromodomain. On the other hand, histone Kcr has been linked to actively transcribed promoters and enhancers in mammalian cells. In light of our observation that CDYL negatively regulates histone Kcr, it is tempting to hypothesize that the downregulation of histone Kcr by CDYL is intrinsically linked to its transcription repression function. Indeed, quantitative chromatin immunoprecipitation (qChIP) showed that the levels of total histone Kcr and H2BK12cr on the promoter of known CDYL target genes *BDNF*, *NEUROD1*, *SCG10*, and *MYT1* (Qi et al., 2014; Zhang et al., 2011) increased significantly in CDYL-KO HeLa cells, whereas the regional level of H3K27me3 in these cells decreased (Figure 3A), as we reported previously (Qi et al., 2014; Zhang et al., 2011). Meanwhile, although histone Kcr was also detected on *HOXA3* promoter, a non-CDYL target (Zhang et al., 2011), its level was not affected by CDYL depletion (Figure 3A), suggesting

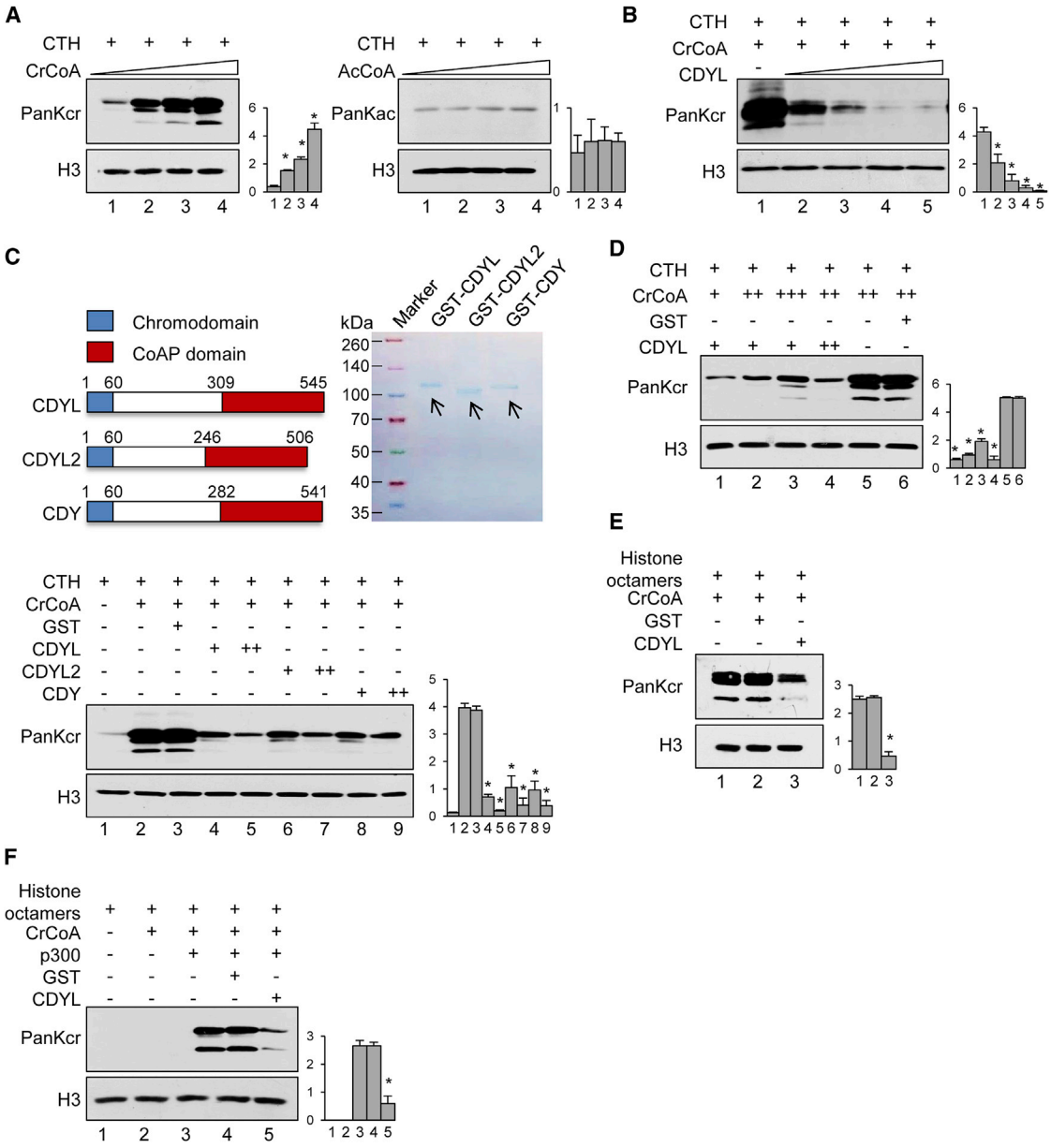

Figure 1. CDYL Negatively Regulates Histone Kcr *In Vitro*

(A) *In vitro* Kcr assays with 5 μg native CTH and 25, 50, 75, or 100 μM crotonyl-CoA or acetyl-CoA. Reaction materials were analyzed by western blotting with pan anti-Kcr or anti-H3.

(B) *In vitro* Kcr assays with 5 μg CTH and 0.05, 0.1, 0.2, or 0.5 μg GST-CDYL in the presence of 50 μM crotonyl-CoA. Reaction materials were analyzed by western blotting with pan anti-Kcr or anti-H3.

(C) *In vitro* Kcr assays with 5 μg CTH and GST-CDYL, GST-CDYL2, or GST-CDY in the presence of 50 μM crotonyl-CoA. Reaction materials were analyzed by western blotting with pan anti-Kcr or anti-H3. Schematic diagrams of CDYL, CDYL2, and CDY and Coomassie brilliant blue (CBB) staining of the purified GST-fused proteins are shown.

(D) *In vitro* Kcr assays with 5 μg CTH and 0.05 or 0.2 μg baculovirally expressed FLAG-CDYL in the presence of 25, 50, or 75 μM crotonyl-CoA. Reaction materials were analyzed by western blotting with pan anti-Kcr or anti-H3. Each scale bar represents the mean ± SD for triplicate experiments. Mean data are normalized to H3 (*$p < 0.05$ versus lane 5).

(E) *In vitro* Kcr assays with 5 μg recombinant *Xenopus* histone octamers and 0.2 μg CDYL in the presence of 50 μM crotonyl-CoA. Reaction materials were analyzed by western blotting with pan anti-Kcr or anti-H3.

(F) *In vitro* Kcr assays with 5 μg recombinant histone octamers and CDYL (0.2 μg), p300 (0.4 μg), and crotonyl-CoA (2 μM). Reaction materials were analyzed by western blotting with pan anti-Kcr or anti-H3. Each scale bar represents the mean ± SD for triplicate experiments. Mean data are normalized to H3 (*$p < 0.05$).

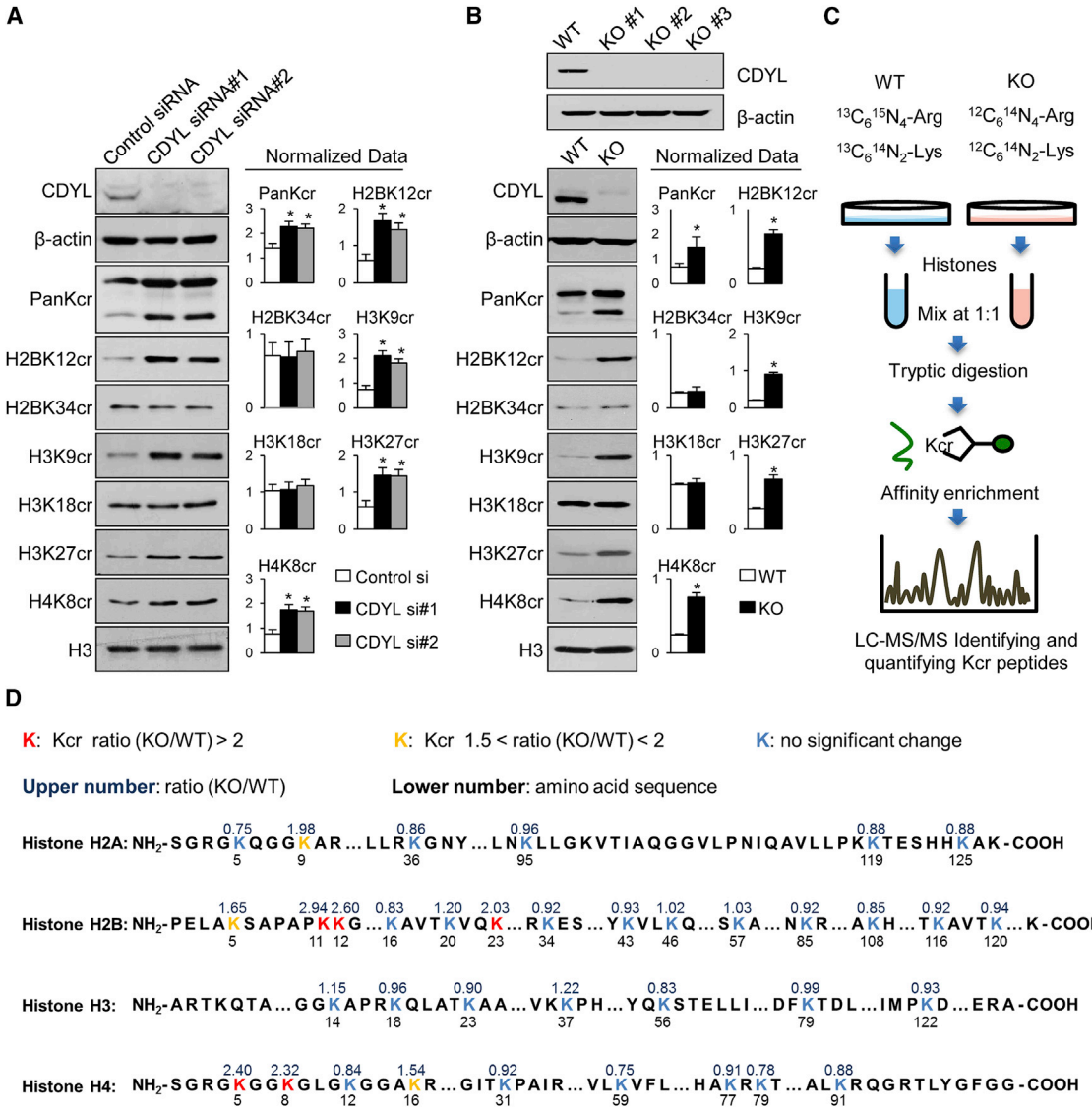

Figure 2. CDYL Negatively Regulates Histone Kcr in Cells

(A) HeLa cells were transfected with CDYL-specific siRNAs and analyzed by western blotting using antibodies against the indicated proteins or histone modifications.

(B) Wild-type (WT) and CDYL-KO (KO) HeLa cells were analyzed by western blotting with antibodies against the indicated proteins or histone modifications. Each scale bar represents the mean ± SD for triplicate experiments. Mean data are normalized to H3 (*$p < 0.05$).

(C) The experimental workflow of the SILAC assays to quantify histone Kcr in wild-type and CDYL-KO HeLa cells.

(D) Histone Kcr sites identified in the SILAC labeling and quantitative proteomics analysis. The histone lysine sites with different changes of the Kcr level are color-coded.

that negative regulation of histone Kcr by CDYL is CDYL target gene specific.

We then investigated whether the chromodomain and thus the chromatin binding is required for negative regulation of histone Kcr by CDYL in cells. To this end, FLAG-tagged full-length CDYL, N terminus (which contains the chromodomain)-deleted CDYL (CDYLΔN), or C terminus (contains the CoAP domain)-deleted CDYL (CDYLΔC) was transfected into CDYL-KO HeLa cells. Protein fractionation assays confirmed that while full-length CDYL and CDYLΔC were largely chromatin bound, CDYLΔN was mainly localized in soluble nuclear fraction (Figure 3B). Ectopic expression of full-length CDYL, but not CDYLΔN and CDYLΔC, was able to rescue CDYL KO-associated alterations of total histone Kcr as well as H2BK12cr and H3K9cr, as measured by immunoblotting (Figure 3C). qChIP assays further showed that only full-length CDYL, but not CDYLΔN and CDYLΔC, could rescue alterations of total histone Kcr and H2BK12cr levels on CDYL target promoters in CDYL-KO HeLa cells (Figure 3D), and qRT-PCR showed that ectopic expression of full-length CDYL, but not CDYLΔN and CDYLΔC, resulted in a

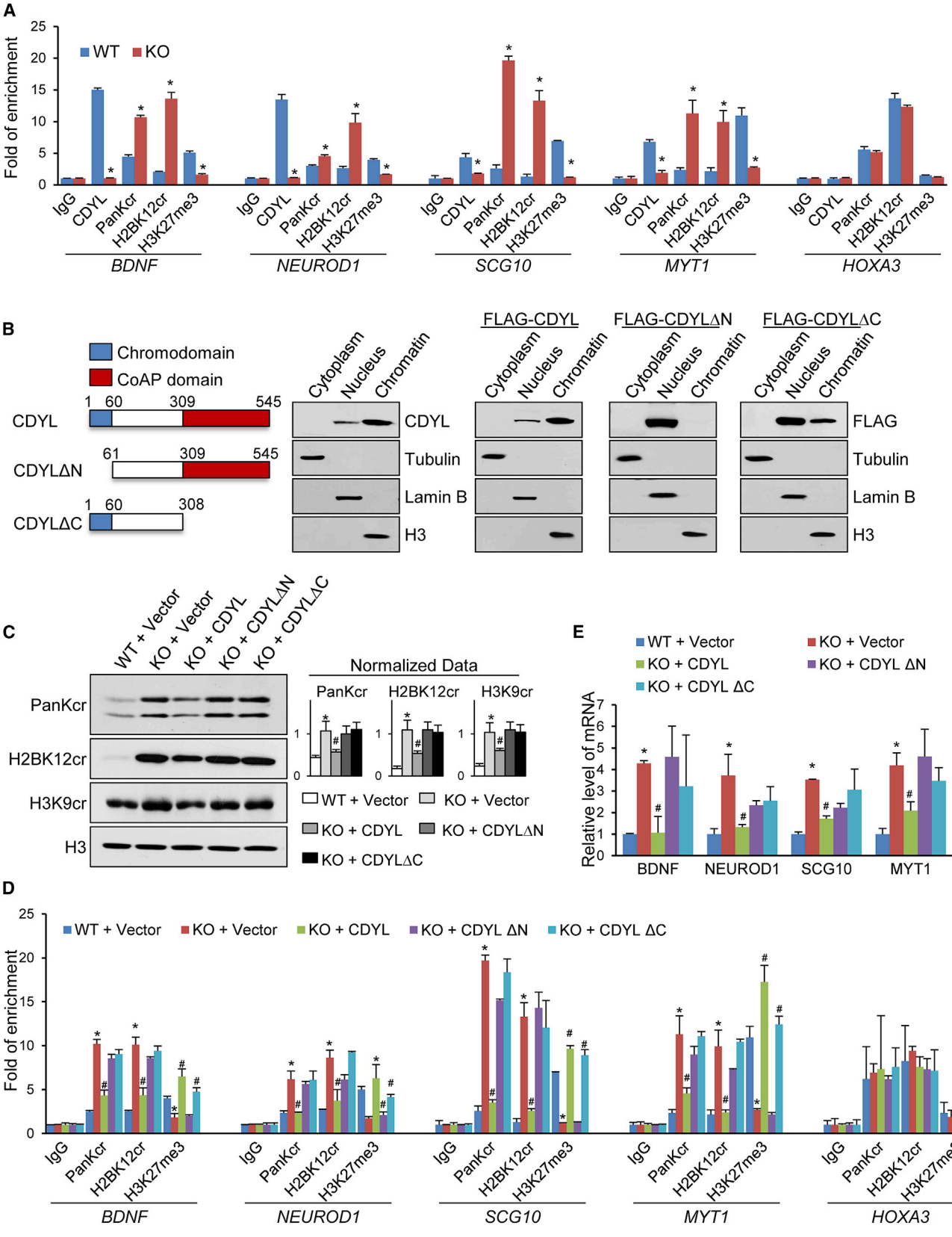

(legend on next page)

decrease in the expression of respective genes (Figure 3E). Together, these results support a notion that both the chromodomain and the CoAP domain of CDYL are required for its negative regulation of histone Kcr.

CDYL Negatively Regulates Histone Kcr by Acting as a Crotonyl-CoA Hydratase

In order to understand the biochemical nature of the negative regulation of histone Kcr by CDYL, we next investigated whether CDYL could act as decrotonylase to directly remove crotonyl groups from histone substrates. *In vitro* fluorometric assays (Tan et al., 2011) were performed first, and the results showed that while recombinant HDAC1 exhibited deacetylation activity toward Boc-Lys(ac)-AMC, recombinant CDYL failed to remove crotonyl moiety from Boc-Lys(cr)-AMC. We tried to add a series of potential cofactors including CoA, acetyl-CoA, Zn^{+}, Ca^{2+}, Mg^{2+}, NAD^{+}, and ATP^{+} to the reaction and found that CDYL still exhibited no catalytic activity toward Boc-Lys(cr)-AMC (Figure S2A). Moreover, immunopurified CDYL from FLAG-CDYL overexpressing HEK293T cells also displayed no decrotonylase activity in the fluorometric assay (Figure S2B).

To determine whether or not CDYL could directly remove Kcr from histone substrates, we synthesized a histone peptide corresponding to amino acid residues 1–21 of H3 with H3K14 being acetylated (H3K14ac) and a histone peptide corresponding to amino acid residues 8–16 of H2B with H2BK12 being crotonylated (H2BK12cr), as both western blotting and LC-MS/MS showed significantly altered level of H2BK12cr upon CDYL depletion (Figure 2). MALDI-TOF-MS revealed that while incubation of the H3K14ac peptide with recombinant HDAC1 resulted in a mass shift corresponding to the acetyl group, incubation of the H2BK12cr peptide with recombinant CDYL had no mass shift (Figure S2C). The inability of CDYL to directly catalyze decrotonylation from H2BK12cr peptide or from oligo-nucleosomal histones was also demonstrated by dot blotting (Figure S2D) and western blotting (Figure S2E), respectively.

The observations that CDYL negatively regulates histone Kcr but could not directly remove crotonyl groups from histone lysine residues prompted us to consider alternative possibilities. In this regard, it is interesting to note that LC-MS showed that CDYL only inhibited the addition of Kcr to new lysine residues, but not those that were already added on CTH (Figure 4A). Similar results were also obtained by immunoblotting of the reaction product, as CDYL only affected histone Kcr when it was incubated with crotonyl-CoA before the addition of CTH (Figure 4B). In addition, a CDYL mutant, CDYLS467A, which is defective in CoA binding (Caron et al., 2003), almost completely lost its ability to inhibit nonenzymatic histone Kcr *in vitro* (Figure 4C). Moreover, recombinant CDYL had no effect on the Kcr level when it was added after bacterially purified histone octamers were crotonylated by p300 *in vitro* (Figure 4D). Together, these data suggest that CDYL acts on crotonyl donor rather than crotonylated histones.

Given that CDYL has a three-dimensional structure that closely resembles that of enoyl-CoA hydratase, a member of the crotonase superfamily (Wu et al., 2009), it is possible that CDYL could also act as a hydratase to destroy crotonyl-CoA for histone Kcr reaction. To test this, we incubated crotonyl-CoA with recombinant GST-CDYL, GST-CDYLΔN, GST-CDYLΔC, GST-CDYLS467A, or control GST protein. MALDI-TOF/TOF-MS analysis of the reaction detected a +18 Da mass shift (equal to that of a H_2O molecule) when crotonyl-CoA was incubated with GST-CDYL and GST-CDYLΔN, but not GST-CDYLΔC, GST-CDYLS467A, or control GST protein (Figure 5A). Further analysis of the mass shifted peak in the reaction containing crotonyl-CoA and GST-CDYL by MALDI-TOF/TOF-MS showed that the mass spectrometric profile of the daughter ions fragmented from the parental ion (m/z 852.1227) matched to that of β-hydroxybutyryl-CoA, confirming crotonyl-CoA hydratation (Figure 5B). Together, these results support a notion that CDYL acts as a crotonyl-CoA hydratase, through its C-terminal CoAP domain, to add a water molecule to the double bond at the position between the second and third carbon atoms of crotonyl-CoA to convert it to β-hydroxybutyryl-CoA. We further determined the steady-state kinetics of the CDYL-catalyzed hydratation reaction by spectrophotometry at different substrate concentrations with the classic mitochondrial metabolic enzyme enoyl-CoA hydratase (ECH) as a positive control. Consistent with previous reports (Agnihotri et al., 2002), the calculated value of K_m and V_{max} of ECH was 14.5 ± 1.44 μM and 36.37 ± 0.95 μM/min, respectively. In comparison, K_m and V_{max} of CDYL was 73.75 ± 16.06 μM and 20.09 ± 2.03 μM/min, respectively (Figure 5C), indicating that the catalytic efficiency of CDYL is lower than mitochondrial ECH. We used triple quadrupole mass spectrometry (QqQ MS) to measure CDYL- or ECH-mediated crotonyl-CoA hydration by quenching the reaction at different time points, and the results confirmed the lower catalytic efficiency of CDYL, compared to that of ECH (Figure 5D).

To gain further support that CDYL acts as a crotonyl-CoA hydratase and inhibits histone Kcr through its influence on the level of cellular crotonyl-CoA in cells, we compared the relative quantitation of crotonyl-CoA and β-hydroxybutyryl-CoA in wild-type

Figure 3. Downregulation of Histone Kcr by CDYL Is Intrinsically Linked to Its Transcription Repression Function

(A) qChIP analysis of Kcr on *BDNF*, *NEUROD1*, *SCG10*, *MYT1* or *HOXA3* promoter in wild-type or CDYL-KO HeLa cells using antibodies against CDYL, pan-Kcr, H2BK12cr, or H3K27me3.

(B) CDYL-KO HeLa cells were transfected with CDYL, CDYLΔN, or CDYLΔC. Total proteins were extracted, fractionated, and analyzed by western blotting with antibodies against the indicated proteins or histone modifications. Schematic diagrams of CDYL, CDYLΔN, and CDYLΔC constructs are shown.

(C) CDYL-KO HeLa cells were transfected with CDYL, CDYLΔN, or CDYLΔC and analyzed by western blotting using antibodies against the indicated proteins or histone modifications. Mean data are normalized to H3.

(D) CDYL-KO HeLa cells were transfected with CDYL, CDYLΔN, or CDYLΔC for qChIP analysis of Kcr on *BDNF*, *NEUROD1*, *SCG10*, *MYT1*, or *HOXA3* promoter with antibodies against the indicated histone modifications.

(E) CDYL-KO HeLa cells were transfected with CDYL, CDYLΔN, or CDYLΔC. The expression of BDNF, NEUROD1, SCG10, and MYT1 was analyzed by qRT-PCR. Each bar represents the mean ± SD for triplicate experiments (*$p < 0.05$ versus WT + Vector; #$p < 0.05$ versus KO + Vector).

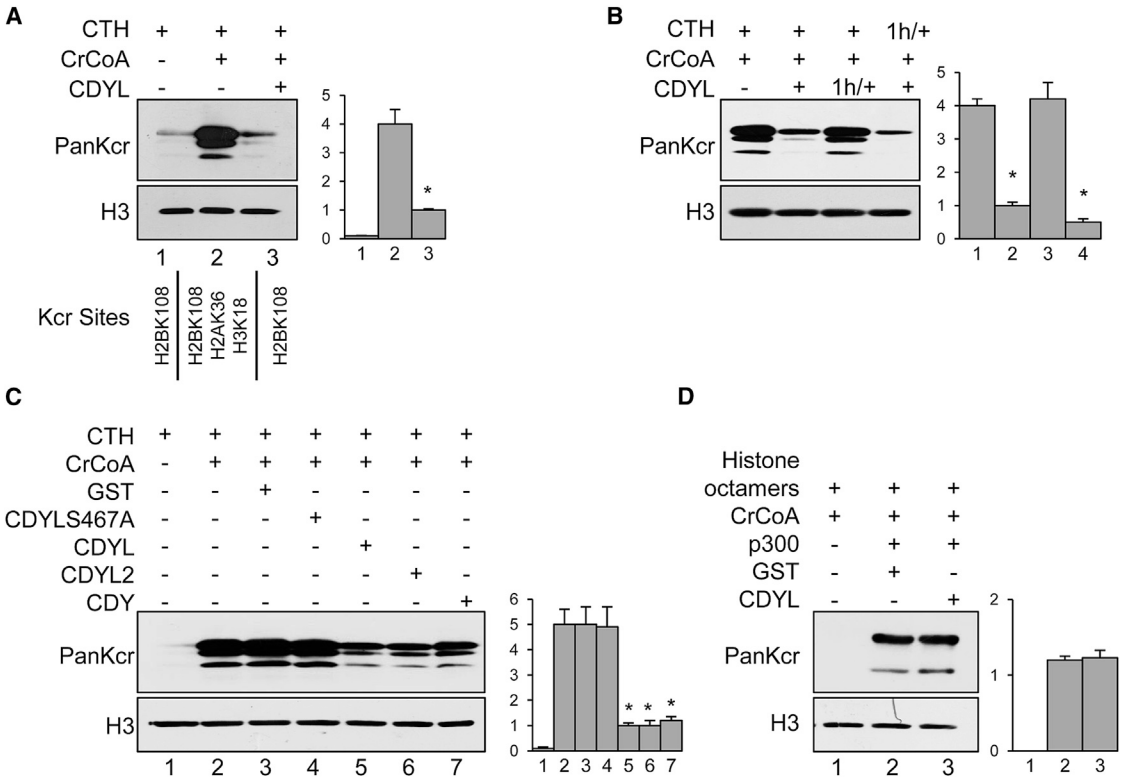

Figure 4. CDYL Acts on Crotonyl Donor rather than Crotonylated Histones

(A) Ten micrograms of CTH were incubated with 50 μM crotonyl-CoA in the presence or absence of 0.2 μg CDYL. The reaction products were subsequently analyzed by western blotting and LC-MS.

(B) Five micrograms of CTH were incubated with 50 μM crotonyl-CoA with addition of CDYL at the beginning of the reaction or 1 hr after as indicated. The reaction mixture was then analyzed by western blotting with pan anti-Kcr or anti-H3.

(C) *In vitro* Kcr assays with 0.2 μg GST-CDYL, GST-CDYL2, GST-CDY, or GST-CDYLS467A in the presence or absence of 50 μM crotonyl-CoA. The reaction mixture was then analyzed by western blotting with pan anti-Kcr or anti-H3.

(D) Five micrograms of recombinant histone octamers were incubated with 0.4 μg p300 and 2 μM crotonyl-CoA, and the reaction was terminated by TCA precipitation. The *in vitro* crotonylated histones were incubated with 0.2 μg CDYL or GST, and the reaction mixture was then analyzed by western blotting with pan anti-Kcr or anti-H3. Mean data are normalized to H3 (n = 3 experiments; *p < 0.05 versus lane 2).

versus CDYL-KO HeLa cells using QqQ MS in selected reaction monitoring (SRM) mode. The results showed that the level of crotonyl-CoA was significantly higher in CDYL-KO HeLa cells than in wild-type HeLa cells (Figure 5E). While the comparable levels of acetyl-CoA were expected, the parallel levels of β-hydroxybutyryl-CoA in wild-type versus CDYL-KO HeLa cells were probably due to the fact that the overall concentration of β-hydroxybutyryl-CoA was buffered off by alternative mechanisms, considering the complexity of cellular metabolic pathways (Figure 5E) (Korman, 2006).

CDYL-Regulated Histone Kcr Is Implemented in Spermatogenesis through Influencing Postmeiotic Gene Reactivation and Histone Replacement

In order to explore the biological significance of CDYL-regulated histone Kcr and to extend our observations to physiologically relevant contexts, we examined the expression of Cdyl and the level of histone Kcr by immunohistochemical staining in a panel of mouse tissues. We found that Cdyl is expressed in heart, pancreas, lung, hippocampus, cortex, and testis and that total histone Kcr and H2B12cr were detected in all of the tissues except thymus, with stronger staining in heart, lung, hippocampus, cortex, and testis (Figure S3), supporting the notion that CDYL-regulated histone Kcr plays a general role in epigenetic regulation, as mentioned earlier.

Of note, both Cdyl (Caron et al., 2003; Lahn et al., 2002) and histone Kcr (Tan et al., 2011) have been implicated in spermatogenesis. However, the underlying molecular mechanisms are poorly understood, and the functional link between Cdyl and histone Kcr has not been reported. qRT-PCR showed that Cdyl expressed at a significantly higher level than Cdyl2 did in the testis, suggesting that Cdyl might be the predominant member of CDY family proteins functioning in mouse testis (Figure 6A). Detailed analysis by immunofluorescent staining and confocal laser scanning microscopy using anti-Cdyl or anti-pan-Kcr revealed that the level of Cdyl expression and the level of histone Kcr in spermatogenic cells exhibited a reversed trend, with Cdyl mainly detected in round spermatids and spermatocytes, while histone Kcr was mainly detected in elongating spermatids (Figure 6B). The pattern of negative correlation between Cdyl expression

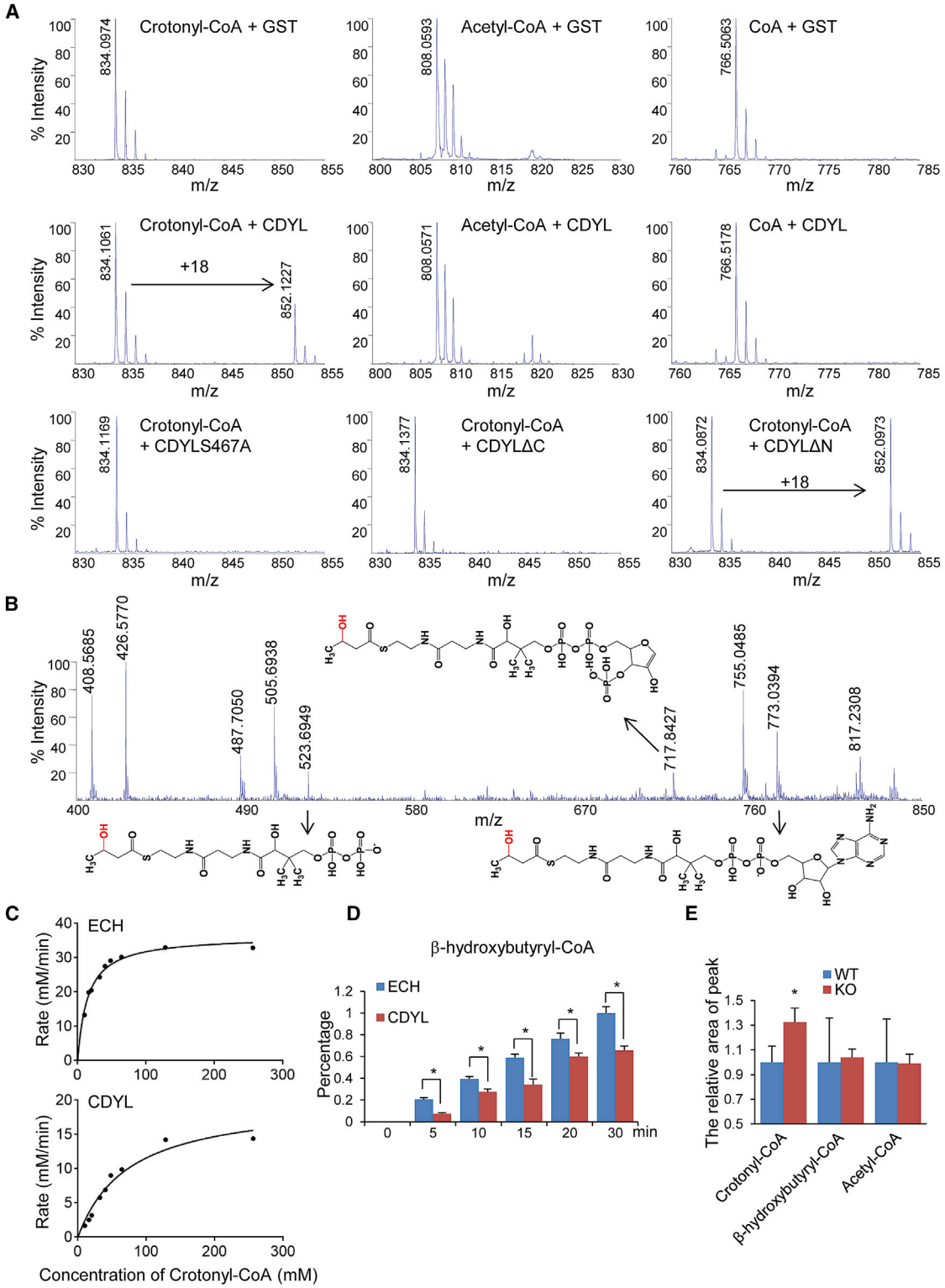

Figure 5. CDYL Negatively Regulates Histone Kcr by Acting as a Crotonyl-CoA Hydratase

(A) Crotonyl-CoA, acetyl-CoA, or CoA (1 μM) was incubated with 0.2 μg recombinant CDYL, CDYL2, CDY, or GST-CDYLS467A for 1 hr at 30°C. The reaction mixture was analyzed by MALDI-TOF/TOF-MS, and the representative spectra are shown.

(legend continued on next page)

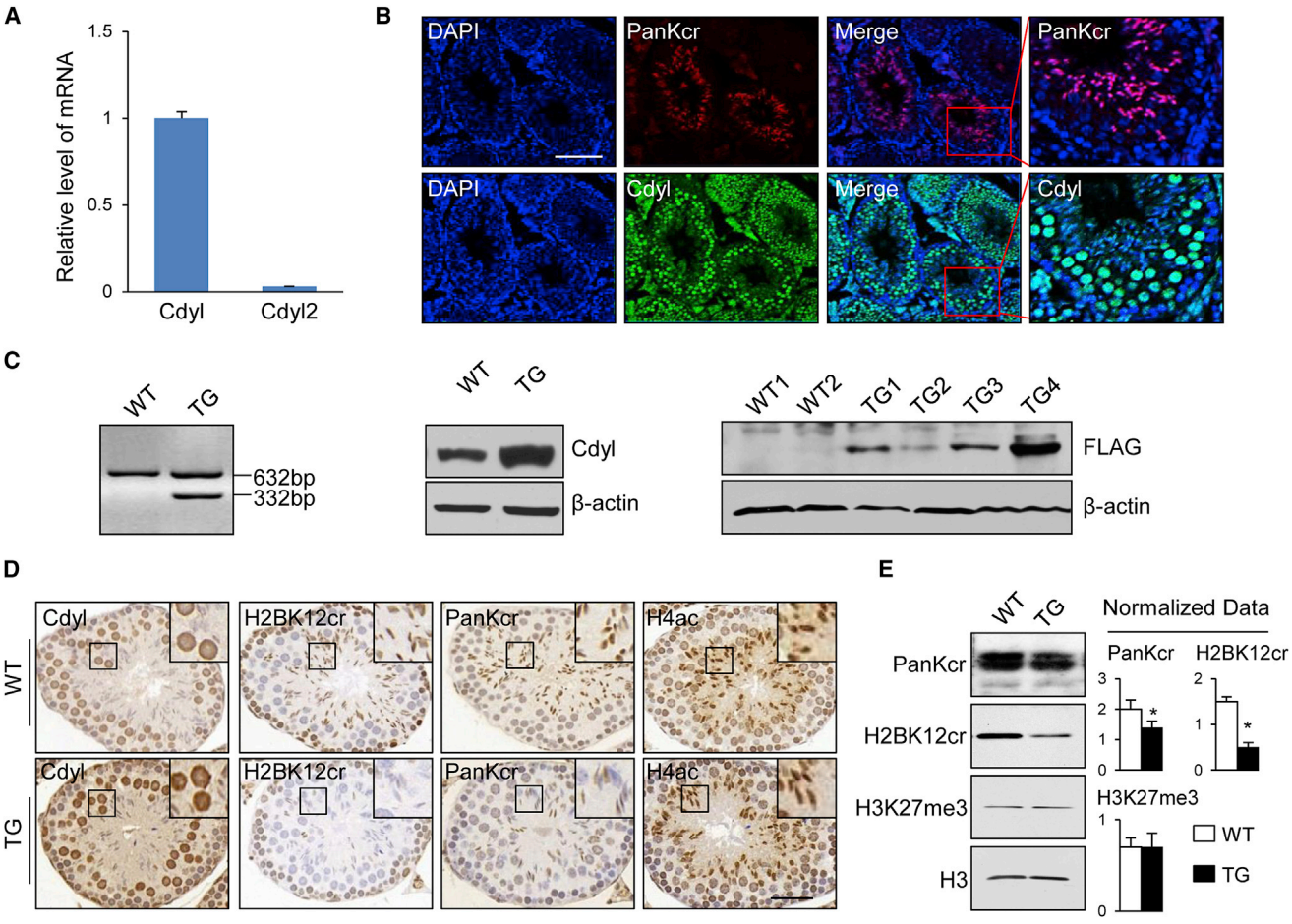

Figure 6. CDYL Negatively Regulates Histone Kcr in Mouse Testes

(A) qRT-PCR analysis of the mRNA levels of Cdyl and Cdyl2 in mouse testes.

(B) Immunofluorescent staining of Cdyl and histone Kcr during mouse spermatogenesis. The stage of seminiferous tubules was XI. Scale bar, 100 μm.

(C) Verification of *Cdyl* transgenic mice by PCR analysis of tail-tip genomic DNA and western blotting of total proteins extracted from the testes.

(D) Immunohistochemical staining of Cdyl and the indicated histone modifications in the testes from wild-type (WT) and *Cdyl* transgenic mice (TG). The stage of seminiferous tubules was XI. Scale bar, 50 μm.

(E) Chromatin histones were extracted from the testes of the WT or TG mice and analyzed by western blotting with antibodies against the indicated protein/histone modifications. Mean data are normalized to H3 (n = 3 experiments; *p < 0.05).

and histone Kcr during spermatogenesis is consistent with our finding that Cdyl negatively regulates histone Kcr.

To better understand the biological function of CDYL in spermatogenesis, we generated *Cdyl* transgenic mice by microinjection of a Cdyl construct into the pro-nuclei of fertilized oocytes, derived from intercross of C57BL/6 × CBA F1 mice (Figure 6C), since it was reported that *Cdyl* knockout mice were embryonically lethal or died shortly after birth (Wan et al., 2013). Immunohistochemical staining with anti-pan-Kcr or anti-H2BK12cr detected significantly reduced levels of histone Kcr in elongating spermatids from *Cdyl* transgenic mice compared to that from wild-type mice, although the level of histone acetylation was

(B) The peak with m/z 852.1227 from MALDI-TOF/TOF-MS in the reaction containing crotonyl-CoA and GST-CDYL was further analyzed by MS/MS analysis. The representative spectra are shown, and the structures of the fragmented irons with m/z 523.6949, 717.8427, and 773.0394 are confirmed by METLIN, a metabolite mass spectral database (https://metlin.scripps.edu).

(C) Crotonyl-CoA (10–300 μM) was quickly mixed with ECH or CDYL (7 nM) and placed in the Thermo Scientific Varioskan Flash. The steady-state kinetics of ECH (upper) or CDYL (lower) were determined by measuring the initial velocities of the reaction, and the data were fit to the Michaelis-Menten equation to determine the values of Km and Vmax for the respective enzymes, as reported in the text.

(D) Crotonyl-CoA (20 μM) was incubated with 7 nM recombinant ECH or CDYL for 0, 5, 10, 15, 20, and 30 min at 30°C. The level of β-hydroxybutyryl-CoA was analyzed by QqQ MS. Mean data are normalized to ECH at 30 min (n = 3 experiments; *p < 0.05).

(E) Cellular levels of crotonyl-CoA, β-hydroxybutyryl-CoA, and acetyl-CoA were measured by QqQ MS. The data were normalized against the level of crotonyl-CoA, β-hydroxybutyryl-CoA, or acetyl-CoA in wild-type HeLa cells. Each bar represents the mean ± SD for triplicate experiments (*p < 0.05).

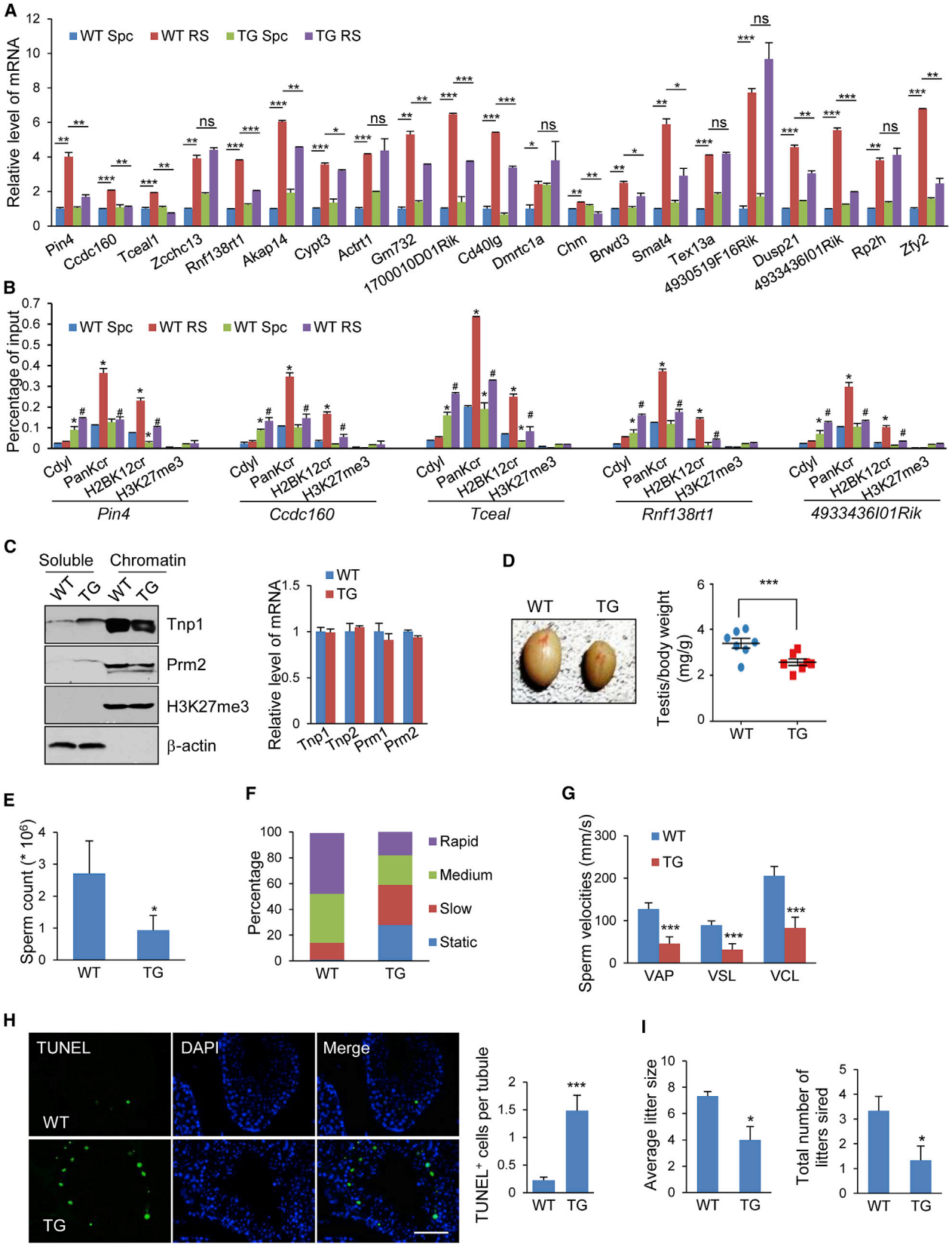

(legend on next page)

comparable (Figure 6D). Similar results were obtained by immunoblotting analysis of mice testes (Figure 6E). These observations are consistent with a role for Cdyl in negative regulation of histone Kcr in mouse testes.

It is proposed that during postmeiotic stages of spermatogenesis, histone Kcr on sex chromosomes marks a subset of genes that escape sex chromosome inactivation after meiosis (Tan et al., 2011). In order to understand the functional significance of Cdyl-regulated histone Kcr in spermatogenesis, we first examined whether the expression of sex chromosome-linked escaped genes was altered in spermatogenic cells in *Cdyl* transgenic mice. To this end, spermatogenic cells from wild-type mice or *Cdyl* transgenic mice were fractionated to enrich spermatocytes (Spc) and postmeiotic round spermatids (RSs), and the expression of the sex chromosome-linked genes was analyzed by qRT-PCR. These genes were chosen based on three criteria: located on the sex chromosomes, having promoters associated with a higher histone Kcr level in RS than Spc, and activated after meiosis, as reported previously (Tan et al., 2011) (GEO DataSets GSM810675 and GSM810678 for ChIP-seq data; GSE217 and GSE4193 for transcriptome data). We found that while these genes expressed comparably in Spc, the majority of them expressed in a greatly reduced level in RS in *Cdyl* transgenic mice, compared to that in wild-type mice (Figure 7A). In addition, qChIP assays detected reduced levels of total histone Kcr and H2BK12cr on the representative promoters in RS of *Cdyl* transgenic mice (Figure 7B). The relative low level of H3K27me3 at the examined X chromosomal promoters in both Spc and RS cells (Figure 7B) is consistent with a previous report showing that H3K27me3 is mainly enriched in autosomes in spermatocytes (Mu et al., 2014). Together, these results support an argument that Cdyl regulates the expression of sex chromosome-linked escaped genes in postmeiotic spermatogenic cells by mainly influencing histone Kcr on the gene promoters.

During spermatogenesis, a unique epigenetic event is genome-wide removal of histones from chromatin and their replacement by transition proteins (Tnps) and protamines (Prms) (Meistrich et al., 2003; Montellier et al., 2013; Oliva, 2006). Although it is reported that histone removal in elongating spermatids is associated with genome-wide hyperacetylation, evidence suggests that other posttranslational histone modifications could also be required to assist this process (Goudarzi et al., 2014; Goudarzi et al., 2016). Given our observation that histone Kcr is highly enriched in elongating spermatids where transcription is essentially ceased, it is possible that histone Kcr might be also involved in histone replacement. To determine whether CDYL-regulated histone Kcr plays a role in histone replacement during spermatogenesis, we examined the levels of chromatin-bound transition proteins and the protamines in testes from wild-type and *Cdyl* transgenic mice. We found that, in testes of wild-type mice, the majority of the transition protein Tnp1 and the protamine Prm2 was chromatin bound, whereas in testes from *Cdyl* transgenic mice, chromatin-associated Tnp1 and Prm2 were significantly reduced and the enrichment of Tnp1 and Prm2 in chromatin-free fraction was significantly elevated (Figure 7C), although qRT-PCR revealed that the mRNA levels of the transition proteins and protamines in testes were comparable between wild-type and *Cdyl* transgenic mice (Figure 7C). These results indicate that histone replacement is dysregulated in the testis of *Cdyl* transgenic mice, which is not due to altered expression of transition proteins or protamines.

In order to further support the role of CDYL-regulated histone Kcr in spermatogenesis, we examined the general function of the testis of *Cdyl* transgenic mice. While *Cdyl* transgenic mice showed no overt differences in body weight from wild-type littermates, they displayed a substantial decrease in the size and weight of the testis (Figure 7D). Significantly, *Cdyl* transgenic mice also exhibited decreased epididymal sperm counts (Figure 7E), sperm cell motility (Figure 7F), and sperm velocity (Figure 7G) and a marked increase in cell apoptosis in the testis (Figure 7H). We finally examined male fertility in *Cdyl* transgenic mice. For this, 11-week-old wild-type male (n = 3) or *Cdyl* transgenic male mice (n = 3) were each bred to two 11-week-old wild-type females, and the number of litters and offspring were counted. Strikingly, during a period of 3 months, the wild-type male mice group produced ten litters with a total of 73 pups, whereas *Cdyl* transgenic male mice group produced only four litters, with a total of 15 pups (Figure 7I). Together, these results

Figure 7. CDYL-Regulated Histone Kcr Is Implemented in Spermatogenesis through Influencing Postmeiotic Gene Reactivation and Histone Replacement

(A) qRT-PCR analysis of the expression of the indicated genes in spermatocytes of wild-type mice (WT Spc), postmeiotic round spermatids of wild-type mice (WT RS), spermatocytes of *Cdyl* transgenic mice (TG Spc), or postmeiotic round spermatids of *Cdyl* transgenic mice (TG RS). Each bar represents the mean ± SD for triplicate experiments (*$p < 0.05$; **$p < 0.01$; ***$p < 0.001$; ns, non-significant).

(B) qChIP analysis of Kcr on *Pin4*, *Ccdc160*, *Tceal*, *Rnf138rt1*, or *4933436I01Rik* promoter in WT Spc, WT RS, TG Spc, or TG RS cells using antibodies against pan-Kcr, H2BK12cr, or H3K23me3. Each bar represents the mean ± SD for triplicate experiments (*$p < 0.05$ versus WT Spc; #$p < 0.05$ versus WT RS).

(C) Soluble or chromatin-bound fractions from WT and TG mouse testes were analyzed by western blotting using antibodies against the indicated proteins or histone modification. The expression of indicated genes in the WT or TG testes was also analyzed by qRT-PCR.

(D) Representative images of the testes from 12-week-old WT or TG mice. The weights of body and testis were also measured and presented as the testis weight per gram of body weight in WT or TG mice (n = 7) (***$p < 0.001$).

(E) Sperms collected from cauda epididymis of 12-week-old WT or TG mice were counted (n = 6) (*$p < 0.05$).

(F) The sperm mobility of 12-week-old WT or TG mice were examined by CASA (Computer-aided Semen Analysis System).

(G) The average path velocity (VAP; μm/s), straight line velocity (VSL; μm/s), and curvilinear velocity (VCL; μm/s) of sperms from 12-week-old WT or TG mice were assessed by CASA (n = 6) (***$p < 0.001$).

(H) TUNEL staining of testis sections from 12-week-old WT or TG mice. Scale bar, 50 μm. The number of apoptotic cells (green) were counted and presented as that per seminiferous tubule in WT or TG mice. Each bar represents the mean ± SD for triplicate experiments (***$p < 0.001$).

(I) Three 11-week-old wild-type male or *Cdyl* transgenic male mice were each bred to two 11-week-old wild-type females, and the number of litters and pups was counted for a period of 3 months (*$p < 0.05$).

indicate that CDYL-regulated histone Kcr plays an important role in spermatogenesis and thus male fertility.

DISCUSSION

Among the newly identified panel of histone acylations, histone Kcr is reported to be associated with active promoters and enhancers in the mammalian genome (Sabari et al., 2015; Tan et al., 2011). In an effort to better understand the regulation of histone Kcr, we investigated the chromodomain protein CDYL, containing an N-terminal chromodomain as a chromatin-presenting module and a C-terminal CoAP domain capable of binding to CoA for its potential crotonyltransferase activity. Surprisingly, contrary to our expectation, our experiments indicate that CDYL regulates histone Kcr negatively. Mechanistically, we showed that CDYL does not catalyze decrotonylation from histones but rather acts as a crotonyl-CoA hydratase to convert crotonyl-CoA to β-hydroxybutyryl-CoA, thereby destroying crotonyl-CoA for histone Kcr reaction. In this regard, it is interesting to note that crystallographic studies revealed that the C-terminal CoAP domain of the CDY family proteins including CDYL has a three-dimensional structure closely resembling enoyl-CoA hydratase (Wu et al., 2009), which catalyzes the hydratation of 2-*trans*-enoyl-CoA into β-hydroxyacyl-CoA in mitochondria during β-oxidation of fatty acids (Bell et al., 2002).

CDYL is known to function as a transcription corepressor (Kim et al., 2006; Vermeulen et al., 2010). Although previous studies indicate that CDYL recruits histone methyltransferases such as PRC2 to facilitate the establishment of repressive modifications such as H3K27me3 at target chromatin region (Zhang et al., 2011), an intrinsic epigenetic regulatory activity for CDYL has not been described, and the enzymatic reaction catalyzed by the C-terminal CoAP domain of CDYL has not been characterized. Thus, how CDYL acts to repress gene transcription is still not fully understood. Since histone hypercrotonylation is associated with active transcription (Sabari et al., 2015; Tan et al., 2011), our finding that CDYL downregulates histone Kcr provides a reasonable account for the transcription-repression function of CDYL. Indeed, we found that both the chromodomain and the CoAP domain of CDYL are required for its negative regulation of histone Kcr, supporting a notion that crotonyl-CoA hydratation catalyzed by CDYL occurs on chromatin when CDYL binds to the genome and that the transcriptional regulatory function of CDYL is intrinsically linked to its negative regulation of histone Kcr.

CDYL-catalyzed negative regulation of histone Kcr is unique in that CDYL acts on crotonyl-CoA donor rather than histone substrates. The biological significance of this kind of epigenetic regulation is not totally clear. Biochemically, unlike acetyl-CoA, crotonyl-CoA contains a carbon-carbon double bond and is thermally unstable. Indeed, accumulating evidence suggests that histone Kcr, as well as some other histone acylations, can take place non-enzymatically when the concentration of cellular crotonyl-CoA is high (Wagner and Hirschey, 2014), and the concentration of crotonyl-CoA also affects histone Kcr catalyzed by specific crotonyltransferase p300 (Sabari et al., 2015). Since CDYL acts on crotonyl-CoA, it could affect both histone crotonyltransferase-dependent or non-enzymatic reactions to prevent spurious histone Kcr that may lead to compromised chromatin configuration and aberrant gene transcription. Notably, we showed that knockout of CDYL in cells is associated with an increase of cellular levels of crotonyl-CoA (Figure 5E). Since CDYL is mainly a nuclear protein bound to chromatin, it is likely that CDYL plays a more profound role in the chromatin surrounding region for the regulation of histone Kcr, although we could not measure nuclear crotonyl-CoA due to its low level or due to technical limitations. As CDYL is an epigenetic regulator capable of binding to the genome and regulating the transcription in a gene-specific manner, it is possible, although purely speculative at this point, that CDYL target genes are evolved such that they are more sensitive to hypercrotonylation. Thus, these genomic targets must be carefully guarded by CDYL to prevent erroneous Kcr in locoregional chromatin. Of note, the eight lysine sites that are targeted by CDYL all locate in the N-terminal tails of core histones. It is possible that these sites are more accessible to regulatory enzymes or to the nuclear environment containing crotonyl-CoA. As mounting evidence suggests that metabolic enzymes might play important roles in transcription regulation by influencing the concentration or availability of essential cofactors for chromatin-modifying enzymes (Sabari et al., 2017; van der Knaap and Verrijzer, 2016), our proposal that CDYL acts as a chromatin methyl-lysine reader while it functions as a crotonyl-CoA sensor offers a direct link between epigenetic regulation and cell metabolism. It is also noteworthy that β-hydroxybutyrylation is also a newly identified histone modification (Xie et al., 2016). Although we did not detect the elevation of β-hydroxybutyryl-CoA accompanied by CDYL-catalyzed hydratation of crotonyl-CoA due to technical limitations or the dynamic nature of biochemical metabolites, it is not unlikely that CDYL-catalyzed hydratation of crotonyl-CoA, at least in part, serves to feed β-hydroxybutyrylation. Future investigations are warranted to delineate the biochemical and functional relationship between histone crotonylation and histone β-hydroxybutyrylation.

During spermatogenesis, the X and Y chromosomes are transcriptionally active during spermatogonial divisions and early meiotic stages but are rapidly silenced in the rest stages of meiosis (Turner, 2007). Intriguingly, some of the sex chromosome-linked genes are reactivated in postmeiotic round spermatids, especially those on the X chromosome (Mueller et al., 2008; Tan et al., 2011), and it is proposed that Kcr on sex chromosomes marks a subset of genes that escape sex chromosome inactivation after meiosis (Tan et al., 2011). Indeed, we showed that histone Kcr is associated with the reactivation of the sex chromosome-linked genes in round spermatids. It is interesting to note that qChIP experiments showed no difference in Cdyl binding at the promoters of the sex chromosome-linked genes between wild-type RS cells and Spc cells, whereas the regional histone Kcr levels in RS cells are significantly higher than those in Spc cells. These observations indicate that the level of histone Kcr during spermatogenesis is likely regulated by multiple mechanisms including both enzymatic and nonenzymatic reactions. Therefore, the differential expression of histone crotonyltransferases and decrotonylases, and the dynamic cellular metabolism which might lead to altered crotonyl-CoA levels in RS cells and Spc cells, could all contribute to the Kcr level at regional chromatin in RS cells being higher than that in Spc cells.

Another major epigenetic event during spermatogenesis in many vertebrate species is the replacement of histones with protamines so that protamines become the primary DNA-packaging protein (Meistrich et al., 2003; Montellier et al., 2013; Oliva, 2006). Although it is believed that the histone replacement in elongating spermatids is associated with genome-wide hyperacetylation, accumulating evidence suggests that additional histone modifications could be involved in the post-meiotic global histone removal (Goudarzi et al., 2014). In support of our observation that CDYL negatively regulates histone Kcr, we found that Cdyl is expressed mainly in the earlier stages of spermatogenesis, whereas hypercrotonylation of histones occurs in elongating spermatids. This pattern of negative correlation between the expression of Cdyl and histone Kcr was also evident in the *Cdyl* transgenic mouse model, in which overexpression of Cdyl was associated with a decrease in histone Kcr in elongating spermatids. In addition, we found that elongating spermatids from *Cdyl* transgenic mice showed compromised histone replacement, supporting a notion that hypercrotonylation facilitates histone replacement. Together, our observations point to an important role for CDYL in the regulation of the major epigenetic events during spermatogenesis. Of note, previous studies indicate that there could be two waves of histone removal: most histones are removed in a process dependent on histone acetylation and the acetyl-lysine reader Brdt, while the remaining histones carrying other histone PTMs such as butyrylation are removed in the second wave, independent of Brdt (Gaucher et al., 2012; Goudarzi et al., 2016). It is possible that CDYL-regulated Kcr is involved in the second wave of histone removal, since recent studies suggest that most bromodomains do not read crotonyl-lysine (Flynn et al., 2015; Li et al., 2016).

In summary, our study identified a biochemical pathway in the regulation of histone Kcr, providing a mechanistic insight into the epigenetic regulatory function of CDYL. Our results indicate that CDYL-regulated histone Kcr is implemented in spermatogenesis, adding to the understanding of the physiology of male reproduction, and may also shed new light on the understanding of how *CDY* deletion on the human Y chromosome might contribute to spermatogenic failure in *AZFc* (*Azoospermia Factor c*)-deleted men.

STAR★METHODS

Detailed methods are provided in the online version of this paper and include the following:

- KEY RESOURCE TABLE
- CONTACT FOR REAGENT AND RESOURCE SHARING
- EXPERIMENTAL MODEL AND SUBJECT DETAILS
  - Cell Culture
  - *Cdyl* Transgenic Mice
- METHOD DETAILS
  - Protein Purification and *In Vitro* Crotonylation Assays
  - *In Vitro* Fluorometric Assays
  - Kinetics Analysis of Crotonyl-CoA Hydratase Activity
  - Cell Transfection
  - TALEN-mediated CDYL Knockout
  - SILAC Labeling and Quantitative Proteomics Analysis
  - Mass Spectrometry Analysis of Acetyl-CoA and Crotonyl-CoA
  - Real-time RT-PCR and ChIP-qPCR
  - Preparation of Nucleosomes
  - Mouse Spermatogenic Cell Fractionation
  - Testis Fractionation Analysis
  - Sperm Cell Count and Motility Analysis
  - Immunohistochemistry and TUNEL Assay
- QUANTIFICATION AND STATISTICAL ANALYSIS
- DATA AND SOFTWARE AVAILABILITY

SUPPLEMENTAL INFORMATION

Supplemental Information includes three figures and one table and can be found with this article at http://dx.doi.org/10.1016/j.molcel.2017.07.011.

AUTHOR CONTRIBUTIONS

S.L., J.L., and Y.S. designed the project, analyzed data, and wrote the manuscript. S.L. conducted most of the experiments. Y.L. constructed CDYL-KO HeLa cells. C.B. and Z.C. conducted and analyzed SILAC experiments. X.L. (Xiaohui Liu) provided technical support and helped with analysis of the QqQ MS experiments. C.H. provided technical support and helped with analysis of the spermatogenesis data. H.Y., X.L. (Xinhua Liu), Y.Z., S.Y., Z.C., G.X., W.L., B.X., J.Y., L.H., T.J., Y.X., and L.S. performed experiments and analyzed data.

ACKNOWLEDGMENTS

This work was supported by grants (91219201 and 81530073 to Y.S., and 31371301 and 81572771 to J.L.) from the National Natural Science Foundation of China and grants (National Key R&D Program of China 2016YFC1302304 to Y.S., and 973 Program 2014CB542004 to J.L.) from the Ministry of Science and Technology of China.

Received: February 1, 2017
Revised: June 2, 2017
Accepted: July 7, 2017
Published: August 10, 2017

REFERENCES

Agnihotri, G., He, S., Hong, L., Dakoji, S., Withers, S.G., and Liu, H.W. (2002). A revised mechanism for the inactivation of bovine liver enoyl-CoA hydratase by (methylenecyclopropyl)formyl-CoA based on unexpected results with the C114A mutant. Biochemistry *41*, 1843–1852.

Bao, X., Wang, Y., Li, X., Li, X.M., Liu, Z., Yang, T., Wong, C.F., Zhang, J., Hao, Q., and Li, X.D. (2014). Identification of 'erasers' for lysine crotonylated histone marks using a chemical proteomics approach. eLife *3*, http://dx.doi.org/10.7554/eLife.02999.

Basu, S.S., and Blair, I.A. (2011). SILEC: a protocol for generating and using isotopically labeled coenzyme A mass spectrometry standards. Nat. Protoc. *7*, 1–12.

Bell, A.F., Feng, Y., Hofstein, H.A., Parikh, S., Wu, J., Rudolph, M.J., Kisker, C., Whitty, A., and Tonge, P.J. (2002). Stereoselectivity of enoyl-CoA hydratase results from preferential activation of one of two bound substrate conformers. Chem. Biol. *9*, 1247–1255.

Caron, C., Pivot-Pajot, C., van Grunsven, L.A., Col, E., Lestrat, C., Rousseaux, S., and Khochbin, S. (2003). Cdyl: a new transcriptional co-repressor. EMBO Rep. *4*, 877–882.

Dorus, S., Gilbert, S.L., Forster, M.L., Barndt, R.J., and Lahn, B.T. (2003). The CDY-related gene family: coordinated evolution in copy number, expression profile and protein sequence. Hum. Mol. Genet. *12*, 1643–1650.

Feldman, J.L., Baeza, J., and Denu, J.M. (2013). Activation of the protein deacetylase SIRT6 by long-chain fatty acids and widespread deacylation by mammalian sirtuins. J. Biol. Chem. *288*, 31350–31356.

Flynn, E.M., Huang, O.W., Poy, F., Oppikofer, M., Bellon, S.F., Tang, Y., and Cochran, A.G. (2015). A subset of human bromodomains recognizes butyryllysine and crotonyllysine histone peptide modifications. Structure *23*, 1801–1814.

Gaucher, J., Boussouar, F., Montellier, E., Curtet, S., Buchou, T., Bertrand, S., Hery, P., Jounier, S., Depaux, A., Vitte, A.L., et al. (2012). Bromodomain-dependent stage-specific male genome programming by Brdt. EMBO J. *31*, 3809–3820.

Goudarzi, A., Shiota, H., Rousseaux, S., and Khochbin, S. (2014). Genome-scale acetylation-dependent histone eviction during spermatogenesis. J. Mol. Biol. *426*, 3342–3349.

Goudarzi, A., Zhang, D., Huang, H., Barral, S., Kwon, O.K., Qi, S., Tang, Z., Buchou, T., Vitte, A.L., He, T., et al. (2016). Dynamic competing histone H4 K5K8 acetylation and butyrylation are hallmarks of highly active gene promoters. Mol. Cell *62*, 169–180.

Kim, J., Daniel, J., Espejo, A., Lake, A., Krishna, M., Xia, L., Zhang, Y., and Bedford, M.T. (2006). Tudor, MBT and chromo domains gauge the degree of lysine methylation. EMBO Rep. *7*, 397–403.

Korman, S.H. (2006). Inborn errors of isoleucine degradation: a review. Mol. Genet. Metab. *89*, 289–299.

Kuroda-Kawaguchi, T., Skaletsky, H., Brown, L.G., Minx, P.J., Cordum, H.S., Waterston, R.H., Wilson, R.K., Silber, S., Oates, R., Rozen, S., and Page, D.C. (2001). The AZFc region of the Y chromosome features massive palindromes and uniform recurrent deletions in infertile men. Nat. Genet. *29*, 279–286.

Lahn, B.T., and Page, D.C. (1999). Retroposition of autosomal mRNA yielded testis-specific gene family on human Y chromosome. Nat. Genet. *21*, 429–433.

Lahn, B.T., Tang, Z.L., Zhou, J., Barndt, R.J., Parvinen, M., Allis, C.D., and Page, D.C. (2002). Previously uncharacterized histone acetyltransferases implicated in mammalian spermatogenesis. Proc. Natl. Acad. Sci. USA *99*, 8707–8712.

Li, X., Liang, J., Yu, H., Su, B., Xiao, C., Shang, Y., and Wang, W. (2007). Functional consequences of new exon acquisition in mammalian chromodomain Y-like (CDYL) genes. Trends Genet. *23*, 427–431.

Li, Y., Sabari, B.R., Panchenko, T., Wen, H., Zhao, D., Guan, H., Wan, L., Huang, H., Tang, Z., Zhao, Y., et al. (2016). Molecular coupling of histone crotonylation and active transcription by AF9 YEATS domain. Mol. Cell *62*, 181–193.

Liu, Y., Liu, S., Yuan, S., Yu, H., Zhang, Y., Yang, X., Xie, G., Chen, Z., Li, W., Xu, B., et al. (2017). Chromodomain protein CDYL is required for transmission/restoration of repressive histone marks. J. Mol. Cell Biol. *9*, 178–194.

Ma, T., Keller, J.A., and Yu, X. (2011). RNF8-dependent histone ubiquitination during DNA damage response and spermatogenesis. Acta Biochim. Biophys. Sin. (Shanghai) *43*, 339–345.

Madsen, A.S., and Olsen, C.A. (2012). Profiling of substrates for zinc-dependent lysine deacylase enzymes: HDAC3 exhibits decrotonylase activity in vitro. Angew. Chem. Int. Ed. Engl. *51*, 9083–9087.

Meistrich, M.L., Mohapatra, B., Shirley, C.R., and Zhao, M. (2003). Roles of transition nuclear proteins in spermiogenesis. Chromosoma *111*, 483–488.

Montellier, E., Boussouar, F., Rousseaux, S., Zhang, K., Buchou, T., Fenaille, F., Shiota, H., Debernardi, A., Héry, P., Curtet, S., et al. (2013). Chromatin-to-nucleoprotamine transition is controlled by the histone H2B variant TH2B. Genes Dev. *27*, 1680–1692.

Mortimer, D., and Mortimer, S.T. (2013). Computer-Aided Sperm Analysis (CASA) of sperm motility and hyperactivation. Methods Mol. Biol. *927*, 77–87.

Mu, W., Starmer, J., Fedoriw, A.M., Yee, D., and Magnuson, T. (2014). Repression of the soma-specific transcriptome by Polycomb-repressive complex 2 promotes male germ cell development. Genes Dev. *28*, 2056–2069.

Mueller, J.L., Mahadevaiah, S.K., Park, P.J., Warburton, P.E., Page, D.C., and Turner, J.M. (2008). The mouse X chromosome is enriched for multicopy testis genes showing postmeiotic expression. Nat. Genet. *40*, 794–799.

Oliva, R. (2006). Protamines and male infertility. Hum. Reprod. Update *12*, 417–435.

Ong, S.E., Blagoev, B., Kratchmarova, I., Kristensen, D.B., Steen, H., Pandey, A., and Mann, M. (2002). Stable isotope labeling by amino acids in cell culture, SILAC, as a simple and accurate approach to expression proteomics. Mol. Cell. Proteomics *1*, 376–386.

Pivot-Pajot, C., Caron, C., Govin, J., Vion, A., Rousseaux, S., and Khochbin, S. (2003). Acetylation-dependent chromatin reorganization by BRDT, a testis-specific bromodomain-containing protein. Mol. Cell. Biol. *23*, 5354–5365.

Qi, C., Liu, S., Qin, R., Zhang, Y., Wang, G., Shang, Y., Wang, Y., and Liang, J. (2014). Coordinated regulation of dendrite arborization by epigenetic factors CDYL and EZH2. J. Neurosci. *34*, 4494–4508.

Sabari, B.R., Tang, Z., Huang, H., Yong-Gonzalez, V., Molina, H., Kong, H.E., Dai, L., Shimada, M., Cross, J.R., Zhao, Y., et al. (2015). Intracellular crotonyl-CoA stimulates transcription through p300-catalyzed histone crotonylation. Mol. Cell *58*, 203–215.

Sabari, B.R., Zhang, D., Allis, C.D., and Zhao, Y. (2017). Metabolic regulation of gene expression through histone acylations. Nat. Rev. Mol. Cell Biol. *18*, 90–101.

Tan, M., Luo, H., Lee, S., Jin, F., Yang, J.S., Montellier, E., Buchou, T., Cheng, Z., Rousseaux, S., Rajagopal, N., et al. (2011). Identification of 67 histone marks and histone lysine crotonylation as a new type of histone modification. Cell *146*, 1016–1028.

Turner, J.M. (2007). Meiotic sex chromosome inactivation. Development *134*, 1823–1831.

van der Knaap, J.A., and Verrijzer, C.P. (2016). Undercover: gene control by metabolites and metabolic enzymes. Genes Dev. *30*, 2345–2369.

Vermeulen, M., Eberl, H.C., Matarese, F., Marks, H., Denissov, S., Butter, F., Lee, K.K., Olsen, J.V., Hyman, A.A., Stunnenberg, H.G., and Mann, M. (2010). Quantitative interaction proteomics and genome-wide profiling of epigenetic histone marks and their readers. Cell *142*, 967–980.

Vogt, P.H., Edelmann, A., Kirsch, S., Henegariu, O., Hirschmann, P., Kiesewetter, F., Köhn, F.M., Schill, W.B., Farah, S., Ramos, C., et al. (1996). Human Y chromosome azoospermia factors (AZF) mapped to different subregions in Yq11. Hum. Mol. Genet. *5*, 933–943.

Wagner, G.R., and Hirschey, M.D. (2014). Nonenzymatic protein acylation as a carbon stress regulated by sirtuin deacylases. Mol. Cell *54*, 5–16.

Wan, L., Hu, X.J., Yan, S.X., Chen, F., Cai, B., Zhang, X.M., Wang, T., Yu, X.B., Xiang, A.P., and Li, W.Q. (2013). Generation and neuronal differentiation of induced pluripotent stem cells in Cdyl−/− mice. Neuroreport *24*, 114–119.

Wu, H., Min, J., Antoshenko, T., and Plotnikov, A.N. (2009). Crystal structures of human CDY proteins reveal a crotonase-like fold. Proteins *76*, 1054–1061.

Xie, Z., Zhang, D., Chung, D., Tang, Z., Huang, H., Dai, L., Qi, S., Li, J., Colak, G., Chen, Y., et al. (2016). Metabolic regulation of gene expression by histone lysine β-hydroxybutyrylation. Mol. Cell *62*, 194–206.

Yang, X., Yu, W., Shi, L., Sun, L., Liang, J., Yi, X., Li, Q., Zhang, Y., Yang, F., Han, X., et al. (2011). HAT4, a Golgi apparatus-anchored B-type histone acetyltransferase, acetylates free histone H4 and facilitates chromatin assembly. Mol. Cell *44*, 39–50.

Zhang, Y., Yang, X., Gui, B., Xie, G., Zhang, D., Shang, Y., and Liang, J. (2011). Corepressor protein CDYL functions as a molecular bridge between polycomb repressor complex 2 and repressive chromatin mark trimethylated histone lysine 27. J. Biol. Chem. *286*, 42414–42425.

STAR★METHODS

KEY RESOURCE TABLE

REAGENT or RESOURCE	SOURCE	IDENTIFIER
Antibodies		
Rabbit polyclonal anti-H2BK12cr	PTM Biolabs	Cat#PTM-509
Rabbit polyclonal anti-H2BK34cr	PTM Biolabs	Cat#PTM-514
Rabbit polyclonal anti-H3K9cr	PTM Biolabs	Cat#PTM-516
Rabbit polyclonal anti-H3K18cr	PTM Biolabs	Cat#PTM-517
Mouse monoclonal anti-H3K27cr	PTM Biolabs	Cat#PTM-526
Rabbit polyclonal anti-H4K8cr	PTM Biolabs	Cat#PTM-522
Rabbit polyclonal anti-PanKcr	PTM Biolabs	Cat#PTM-501
Rabbit polyclonal anti-PanKac	PTM Biolabs	Cat#PTM-105
Rabbit polyclonal anti-CDYL	Sigma	Cat#SAB2500224
Rabbit polyclonal anti-H3	Abcam	Cat#ab1791
Mouse monoclonal anti-actin	Abcam	Cat#ab8226
Mouse monoclonal anti-FLAG	Abcam	Cat#ab49763
Rabbit polyclonal anti-H4ac	Active Motif	Cat#39243
Rabbit polyclonal anti-Prm2	Proteintech	Cat#14500-1-AP
Rabbit polyclonal anti-Tnp1	Proteintech	Cat#17178-1-AP
Rabbit polyclonal anti-H3K27me3	Millipore	Cat#ABE44-S
Rabbit polyclonal anti-CDYL	This paper	N/A
Bacterial and Virus Strains		
DH5 *Escherichia coli*	Transgen Biotech	CD201-01
BL21 *Escherichia coli*	Transgen Biotech	CD601-01
Chemicals, Peptides, and Recombinant Proteins		
Human p300 protein	Sigma	Cat#SRP8022
Protein A Sepharose CL-4B beads	GE Healthcare Bioscience	Cat#17-0963-03
protease inhibitor cocktail	Roche	Cat#04 693 132 001
Boc-Lys(crotonyl)-AMC	Dr. Yingming Zhao Lab (University of Chicago)	N/A
Boc-Lys(acetyl)-AMC	Dr. Yingming Zhao Lab	N/A
Crotonyl coenzyme A	Sigma	Cat#A2056
Acetyl coenzyme A	Sigma	Cat#28007
Coenzyme A	Sigma	Cat#C4282
β-Hydroxybutyryl Coenzyme A	Sigma	Cat#H0261
H2B8-16K12cr peptides	This paper	N/A
H31-21K14ac peptides	This paper	N/A
Xenopus histone	Zhang et al., 2011	N/A
Lipofectamine 2000	Invitrogen	Cat#11668019
LipofectamineTM RNAiMAX	Invitrogen	Cat#13778100
13C615N4-arginine (Arg-10)	Thermo	Cat#89990
13C614N2-lysine (Lys-6)	Thermo	Cat#89988
12C614N4-arginine (Arg-0)	Thermo	Cat#88427
12C614N2-lysine (Lys-0)	Thermo	Cat#88429
C18 ZipTips	Millipore	Cat#ZTC18M960
Bovine liver enoyl-CoA hydratase (ECH)	This paper	N/A

(*Continued on next page*)

Continued

REAGENT or RESOURCE	SOURCE	IDENTIFIER
Deposited Data		
METLIN database	The original and most comprehensive MS/MS metabolite database	http://metlin.scripps.edu/
Raw data	Mendeley	http://dx.doi.org/10.17632/gbb7r6gg5v.1
Experimental Models: Cell Lines		
Human: HeLa cells	ATCC	CCL-2
Human: CDYL-KO HeLa cells	This paper	N/A
Spodoptera frugiperda: Sf9 cells	ATCC	CRL-1711
Experimental Models: Organisms/Strains		
Mouse: C57BL/6	Beijing Vital River Laboratory Animal Technology Co., Ltd.	Strain number: 213
Mouse: Cdyl transgenic C57BL/6	This paper	N/A
Oligonucleotides		
siRNA targeting sequence: CDYL-siRNA#1 sense: CAGAGAAUAACUCACUAAAdTdT	This paper	N/A
siRNA targeting sequence: CDYL-siRNA#1 antisense: UUUAGUGAGUUAUUCUCUGdTdT	This paper	N/A
siRNA targeting sequence: CDYL-siRNA#2 sense: GAGAUAUUGUGGUCAGGAAtt	This paper	N/A
siRNA targeting sequence: CDYL-siRNA#2 antisense: UUCCUGACCACAAUAUCUCtt	This paper	N/A
Primers used for Real-time RT-PCR, see Table S1	This paper	N/A
Primers used for ChIP-qPCR, see Table S1	This paper	N/A
Recombinant DNA		
pET42a-CDY	This paper	N/A
pET42a-CDYL	This paper	N/A
pET42a-CDYL2	This paper	N/A
pET42a-CDYL-S467A	This paper	N/A
pET42a-HDAC1	This paper	N/A
TALEN-CDYL-L	This paper	N/A
TALEN-CDYL-R	This paper	N/A
Software and Algorithms		
Computer Assisted Semen Analysis (CASA) system	Hamilton Thorne	N/A
SkanIt RE for Varioskan Flash	Thermo software	N/A
ImageJ64	NIH	https://imagej.nih.gov/ij/
GraphPad Prism 6	GraphPad software	N/A
Other		
FastTALETM TALEN assembly kit	SIDANSAI Biotechnology	Cat#1802-030
Reverse Transcription System	Roche	Cat#11117831001
QIA quick PCR Purification Kit	QIAGEN	Cat#28106
2 × Premix Taq	TaKaRa	Cat#R004Q
DAB Detection Kit	Gene Tech	Cat#: 347010
Nuclei PURE Prep kit	Sigma-Aldrich	Cat#NUC201

CONTACT FOR REAGENT AND RESOURCE SHARING

Further information and requests for reagents may be directed to, and will be fulfilled by, the Lead Contact, Dr. Yongfeng Shang (yshang@hsc.pku.edu.cn).

EXPERIMENTAL MODEL AND SUBJECT DETAILS

Cell Culture

HeLa cells were maintained in Dulbecco's Modified Eagle's Medium (DMEM) (Hyclone) supplemented with 10% fetal bovine serum (FBS) and penicillin and streptomycin, under 5% CO_2.

Cdyl Transgenic Mice

Cdyl transgenic mice were generated by Cyagen Biosciences. For transgenesis, ORF of mouse Cdyl (1806bp) with a FLAG tag was cloned into the mammalian expression vector pRP.Des2d. After digestion with *Not* I, linearized DNA was used for microinjection into the pro nuclei of fertilized oocytes, derived from intercrosses of (C57BL/6 × CBA) F1 mice. Transgenic mice were identified by PCR of tail-tip genomic DNA. The transgene PCR sense and antisense primers were 5′-GCTTTTGGAGTACGTCGTCT −3′ and 5′-GCAGGTGTTATCATCAGTAGGTT −3′, respectively. The internal control PCR sense and antisense primers were 5′-CAACCACT TACAAGAGACCCGTA-3′ and 5′-GAGCCCTTAGAAATAACGTTCACC-3′, respectively. Amplification of the transgene and internal control resulted in PCR products of 332 bp and 632 bp, respectively. Briefly, 2 μl of genomic DNA was amplified in 2 × Premix Taq (TaKaRa), 0.8 μl of each transgene primer and 0.4 μl of each internal primer in a total volume of 25 μl. After an initial denaturation at 94°C for 3 min, samples were amplified for 38 cycles (94°C for 30 s, 57°C for 35 s, 72°C for 35 s). After the last cycle, samples were incubated for 5 min at 72°C and resolved in 2% TAE-agarose gels. Two founder mice with similar Cdyl overexpressing levels were mated with wild-type C57BL/6 mice to obtain the F1 generation. Animal handling and procedures were approved by the Institutional Animal Care of Peking University Health Center.

METHOD DETAILS

Protein Purification and *In Vitro* Crotonylation Assays

pET42a constructs containing GST-His fused CDYL, CDYL2, CDY, CDYL-S467A, HDAC1 or ECH were expressed in BL21 *Escherichia coli*. Protein expression was induced by adding isopropyl β-D-1-thiogalactopyranoside to a final concentration of 0.4 mM when OD600 reached 0.6, and the culture was further grown at 30°C for 6 hr. Cells were harvested and resuspended in lysis buffer A (50 mM Tris-HCl, pH 7.5, 300 mM NaCl, 1 mM PMSF, and Roche EDTA free protease inhibitor). Following sonication and centrifugation, the supernatant was loaded onto a nickel column pre-equilibrated with lysis buffer. The column was washed with 5 column volumes of wash buffer (lysis buffer with 20 mM imidazole) and the bound proteins were then eluted with elution buffer (lysis buffer with 500 mM imidazole). After purification, proteins were dialyzed at 4°C overnight. Purification of recombinant *Xenopus* histone octamers and baculoviral production of CDYL protein were described previously (Zhang et al., 2011).

For *in vitro* enzymatic reactions, 5 μg native CTHs or recombinant *Xenopus* histone octamers were incubated with 0.2 μg recombinant CDYL protein at 30°C for 1 hr in buffer A (50 mM Tris pH 8.0, 10% glycerol, 1 mM DTT, 0.2 mM PMSF) unless otherwise stated. The assay mixture was then analyzed using western blotting or LC-MS/MS system. Alternatively, 200 ng $H2B_{8-16}$K12cr and $H3_{1-21}$K14ac peptides were incubated with 0.2 μg recombinant CDYL or HDAC1 protein at 30°C for 1 hr in buffer A and the assay mixture was subsequently analyzed using MALDI-TOF/TOF mass spectrometer (ABSciex, Canada). Otherwise, 1 μM crotonyl-CoA, acetyl-CoA, or CoA was incubated with 0.2 μg recombinant CDYL or GST at 30°C for 1 hr in buffer A followed by analyzing with MALDI-TOF/TOF-MS, in which negative ion mode was used to collect the spectra due to its lower background. The peak with mass-to-charge (m/z) ratio 852.1227 was further fragmented in negative ion mode for structural confirmation using MALDI-TOF/TOF. Metabolite identification was performed by matching MS/MS spectrum with METLIN database (http://metlin.scripps.edu/) with mass tolerance of ± 0.1 Da.

In Vitro Fluorometric Assays

Reactions were performed in a final volume of 50 μL per well in a 96-well microplate as described (Tan et al., 2011). Briefly, 1 μL of Boc-Lys(crotonyl)-AMC stocking solution (10 mM) and 200 ng recombinant CDYL protein (or 2 μg FLAG-CDYL complex purified from HeLa cells) was added to the reaction buffer (25 mM Tris·HCl, 130 mM NaCl, 3 mM KCl, 1 mM $MgCl_2$, 0.1% PEG8000, pH = 8.0) and incubated at 37°C for 3 hr. 1 mM of various potential cofactors, including CoA, acetyl-CoA, Zn^+, Ca^{2+}, Mg^{2+}, Nicotinamide Adenine Dinucleotide (NAD^+), or ATP, were added in the reaction mixture as indicated. The reaction was then stopped by adding 25 μL of trypsin solution (25 mM Tris·HCl, 130 mM NaCl, 3.0 mM KCl, 1 mM MgCl, 30% isopropanol, 0.01 mg/mL trypsin, [pH = 8.0]). The resulting solvent was mixed and incubated at 37°C for another 1 hr. The fluorescence was analyzed by a fluorescence plate reader (The Wallac 1420 Workstation, IET Ltd, Vernon Hills, IL) with excitation and emission wavelengths at 355 nm and 460 nm, respectively.

Kinetics Analysis of Crotonyl-CoA Hydratase Activity

Bovine liver ECH was purified from *E. Coli*, and hydratase activity of ECH and CDYL toward crotonyl-CoA was determined by spectrophotometric measurement of the absorbance at 263 nm which corresponds to the α, β-unsaturated enoyl moiety of the substrate (Agnihotri et al., 2002). The assay cocktail consisted of 50 mM potassium phosphate, 3 mM EDTA (pH 7.5), and crotonyl-CoA (10-300 μM) in a total volume of 200 μl. The reaction was initiated by the addition of ECH or CDYL (7 nM), after which the contents

were quickly mixed and placed in the Thermo Scientific Varioskan Flash. The steady-state kinetic parameters of ECH and CDYL were determined by measuring the initial velocities of the reaction and the data were fit to the Michaelis-Menten equation to determine the values of Km and Vmax for the respective enzymes.

Crotonyl-CoA (20 μM) was incubated with 7nM recombinant ECH or CDYL for 0, 5 and 10min at 30°C. Reactions were terminated by addition of 40 μL reaction mixture into a tube containing 10 μL. The measurement was performed by UPLC coupled triple quadrupole mass spectrometer (TSQ Quantiva, Thermo). Data were acquired in SRM for β-hydroxybutyryl-CoA and crotonyl-CoA with transitions of 852/408 (ESI-) and 836/329 (ESI+), respectively. Data analysis and quantitation were performed by the software Xcalibur 3.0.63 (Thermo Fisher, CA).

Cell Transfection

All transfections were carried out using Lipofectamine 2000 (Invitrogen) according to the manufacturer's recommendations. Cells were transfected with siRNA oligonucleotides using Lipofectamine™ RNAiMAX (Invitrogen) with the final concentration at 20 nM.

TALEN-mediated CDYL Knockout

A TALEN binding pair was chosen from CDYL gene in the second exon between GTT222964 and AAG223630 (total 667 bp), as the first exon of CDYL is too short (total 24 bp). The genomic recognition sequences of TALEN left and right arms are GAGGAATACATC CACGAC (L) and GCTCTCCTTCTGCTTCTC (R), spaced by 16 bp and anchored by a preceding T base at the −1 position to meet the optimal criteria for natural TAL proteins (Liu et al., 2017). TALEN vectors of left and right arms, TALEN-CDYL-L and TALEN-CDYL-R, were obtained by one-step ligation using FastTALE™ TALEN assembly kit (SIDANSAI Biotechnology) according to the manufacturer's instructions. HeLa cells were transfected with the two TALEN-CDYL vectors. Puromycin-resistant cell clones were analyzed by PCR and DNA sequencing was performed to confirm CDYL deletion.

SILAC Labeling and Quantitative Proteomics Analysis

SILAC labeling and quantitative proteomics analysis was performed as previously described (Ong et al., 2002). Briefly, wild-type or CDYL-KO HeLa cells were grown in Dulbecco's modified Eagle's medium supplemented with 10% fetal bovine serum and either the "heavy" form $^{13}C_6{}^{15}N_4$-arginine (Arg-10) and $^{13}C_6{}^{14}N_2$-lysine (Lys-6) or "light" from $^{12}C_6{}^{14}N_4$-arginine (Arg-0) and $^{12}C_6{}^{14}N_2$-lysine (Lys-0) respectively. The cells were grown for more than six generations before being harvested to achieve more than 97% labeling efficiency. After that, the cells were further expanded in SILAC media to desired cell number (~5×10^8) in 15 × 150 mm^2 plates. The cells were then collected and the core histones were isolated and digested with trypsin. Lysine crotonylation (Kcr) peptides were then enriched by pre-washed antibody beads (PTM Biolabs, Hangzhou). The eluted peptides were cleaned with C18 ZipTips (Millipore) according to the manufacturer's instructions, followed by analysis with LC-MS/MS. The resulting MS/MS data were processed by using MaxQuant with integrated Andromeda search engine (version 1.5). False discovery rate thresholds for protein, peptide and modification sites were specified at 1%. The cutoff of significant fold-change of histone crotonylation between CDYL-KO cells and wild-type HeLa cells was set with a quantitative ratio above 1.5 or below 0.67.

Mass Spectrometry Analysis of Acetyl-CoA and Crotonyl-CoA

The acyl-CoA extraction procedure was based upon previously described (Basu and Blair, 2011) method with minor modifications. Cultured HeLa cells from 5 × 150 mm plates were washed once with cold deionized water and metabolites were extracted by the addition of 1 mL ice cold 10% trichloroacetic acid (TCA). Following 15 s incubation on ice, cells were collected by scrapping and transferred to a 1.5 mL tube. Cell extracts were sonicated for 3 × 30 s (Bioruptor, Diagenode) and then centrifuged at 14,000 rpm for 5 min at 4°C to remove protein. Acyl-CoAs were further purified using a HLB solid phase extraction column and vacuum manifold. SPE columns were conditioned with 1 mL methanol, and equilibrated with 1 mL water. Supernatants were applied and SPE columns were then washed with 1 mL water; acyl-CoAs were eluted using three successive applications of 0.5 mL methanol containing 25 mM ammonium acetate. Eluted acyl-CoAs were dried for 3 hr in a bench top solvent evaporator. Dried samples were stored at −80°C and re-suspended in 100 μL 5% 5-sulfosalicylic acid (SSA) immediately prior to analysis by triple quadrupole mass spectrometry (QqQ MS). Data acquisition was performed in selected reactions monitoring (SRM) mode with transitions of 810/303 (ESI+) and 836/329 (ESI+) for acetyl-CoA and crotonyl-CoA. Commercial CoAs were used as the standard for quantification reference. In the analysis, a reversed phase liquid chromatography (RPLC) method was utilized with 5 mM trimethylamine, 3 mM acetate in water and 100% methanol as mobile phase A and B respectively. A 15 min gradient from 5% to 90% mobile B was applied for crotonyl-CoA, hydroxybutyryl-CoA and acetyl-CoA.

Real-time RT-PCR and ChIP-qPCR

Total cellular RNAs were isolated with the TRIzol reagent (Invitrogen) and used for the first strand cDNA synthesis with the Reverse Transcription System (Roche). Quantitation of all gene transcripts was done by qPCR using Power SYBR Green PCR Master Mix and an ABI PRISM 7500 sequence detection system (Applied Biosystems, Foster City, CA) with the expression of GAPDH as the internal control. ChIP experiments were performed according to the procedure described previously (Zhang et al., 2011). DNA was purified with the QIAquick PCR Purification Kit. Primers are listed in Table S1.

Preparation of Nucleosomes

Nucleosomes were prepared according to protocols described previously (Yang et al., 2011). Briefly, Permeabilized nuclei from HeLa cells were prepared and digested with 2.5 units/ml MNase. Nucleosomes were then purified by sucrose gradient. Genomic DNA was purified and resolved by agarose gel electrophoresis to visualize mono-, di-, and tri-nucleosomes.

Mouse Spermatogenic Cell Fractionation

Spermatogenic cell fractionation was carried out by sedimentation of total germ cells on a BSA gradient as previously described (Pivot-Pajot et al., 2003). Cell fractions were controlled by visual inspections for the enrichment assessment. Each sedimentation experiment used 6 mouse testes and the respective fractions corresponding to spermatocytes and round spermatids from 10 fractionation experiments were pooled for subsequent real time RT-PCR and ChIP experiments. The enrichments in spermatocytes and round spermatids obtained in the corresponding fractions were 80% and 85%, respectively.

Testis Fractionation Analysis

For western blotting of mouse testis, the cell pellet was lysed with NETN (50 mM Tris-HCl [pH 8.0], 100 mM NaCl, 2 mM EDTA, and 0.5% NP-40) (Ma et al., 2011). After centrifugation, the soluble fraction was collected and the pellet was treated with 0.2 N HCl to release chromatin-bound proteins, which were then neutralized using 2N NaOH. Both fractions were analyzed by western blotting with antibodies against the indicated proteins.

Sperm Cell Count and Motility Analysis

To obtain the sperm cell count, the entire epididymis from the mouse was minced in a sperm washing medium and incubated for 30 min at 37°C. Total epididymal sperm cell counts and motility were evaluated using the Computer Assisted Semen Analysis (CASA) system (Hamilton Thorne, USA) (Ma et al., 2011; Mortimer and Mortimer, 2013).

Immunohistochemistry and TUNEL Assay

Immunohistochemistry was performed on tissues paraffin sections similarly as previously described (Tan et al., 2011). Mouse tissues were incubated with indicated antibodies and positively stained cells were then visualized using the DAB Detection Kit (Gene Tech, Shanghai, China) according to the manufacturer's instructions. Following counterstaining with nuclear hematoxylin, images were captured under a microscope. TUNEL assays were performed with the In Situ Cell Death Detection Fluorescein Kit (Roche), following the manufacturer's instruction. Mouse tissues were incubated with TUNEL reaction mixture and followed with DAPI staining to visualize DNA. The images were captured under a fluorescence microscope.

QUANTIFICATION AND STATISTICAL ANALYSIS

Group data are presented as mean ± SD. Comparisons between two groups were made by Student's paired or unpaired two-tailed t tests where it is appropriate. *P value*s less than 0.05 were considered significant. Analyses were performed using the Microsoft Excel and GraphPad Prism V6.0.

DATA AND SOFTWARE AVAILABILITY

Raw data have been deposited to Mendeley Data and are available at http://dx.doi.org/10.17632/gbb7r6gg5v.1.